1 # New Technologies can Cost-effectively Reduce Oil and
2 # Gas Methane Emissions, but Policies will Require Careful
3 # Design to Establish Mitigation Equivalence
4
5 Chandler Kemp and Arvind P. Ravikumar
6
7 Email: ckemp@harrisburgu.edu, aravikumar@harrisburgu.edu
8 Twitter: @arvindpawan1
9
10 Department of Systems Engineering, Harrisburg University of Science and
11 Technology, Harrisburg PA 17101
12
13 ## Abstract:
14 Reducing methane emissions from oil and gas systems is a central component of US and
15 international climate policy. Leak detection and repair (LDAR) programs using optical gas
16 imaging (OGI) based surveys are routinely used to mitigate fugitive emissions or leaks.
17 Recently, new technologies and platforms such as planes, drones, and satellites promise more
18 cost-effective methane mitigation than existing approaches. To be approved for use in LDAR
19 programs, new technologies must demonstrate equivalent emissions mitigation to existing
20 approaches. In this work, we use the FEAST modeling tool to (a) identify cost vs. mitigation
21 trade-offs that arise from the use of new technologies, and (b) provide a framework for effective
22 design of alternative LDAR programs. We identify several critical insights. First, new
23 technologies and tiered LDAR programs can achieve equivalent emissions reductions at lower
24 cost as current OGI-based approaches by varying survey frequency. Second, low median
25 detection threshold technologies can trade sensitivity for speed without sacrificing mitigation
26 outcomes. Third, emissions mitigation from technologies with high median detection thresholds
27 have an effective upper bound independent of the survey frequency. Finally, vented emissions
28 play a critical role in the cost-effectiveness of tiered detection programs that direct ground crews
29 based on site-level emissions detection. The FEAST model will enable operators and regulators
30 to systematically evaluate the role of new technologies in next generation LDAR programs.
31
32
33
34
35
36
37
38
39
40
41

1   Introduction

Methane emissions from petroleum and natural gas systems accounted for 28% of US methane emissions in 2018, based on the Environmental Protection Agency's (EPA) greenhouse gas inventory (GHGI) [1]. Furthermore, several recent studies have shown that official GHGI estimates likely underestimate methane emissions from natural gas systems [2–6]. Methane is the primary constituent of natural gas and has a global warming potential 34 times greater than that of carbon dioxide over 100 years [2]. Therefore, reducing methane emissions from oil and gas operations is critical to realize GHG emissions benefits from recent coal-to-gas fuel switching in the power sector [7]–[9]. In addition, addressing methane emissions reduces volatile organic compounds co-emitted from natural gas production facilities, thereby improving local air quality [10]. Most importantly, minimizing methane leakage is necessary to achieve long-term climate targets. Gas production continues through 2040 in all pathways considered by the Intergovernmental Panel on Climate Change (IPCC) Special Report on global warming of 1.5°C, and persists at greater than 20% of the 2010 production rate in 75% of pathways [11], [12]. Regardless of whether the combustion emissions associated with this production can be mitigated by carbon capture and storage, eliminating upstream methane emissions is necessary to avoid the most severe effects of climate change.

State and federal governments throughout North America have enacted regulations in recent years to address methane emissions from oil and gas activity. California, Colorado, Pennsylvania and several other states now require periodic leak detection and repair (LDAR) programs at upstream and midstream facilities to find and fix leaks [11–15]. Separately, some oil and gas companies have also implemented voluntary LDAR programs to reduce methane leakage from their operations [18]. The most common technologies approved by regulators and used in these LDAR programs include EPA's Method-21 and optical gas imaging (OGI) based infrared cameras. Recent field work has shown that these OGI-based LDAR surveys have been effective in reducing emissions over several years [18]. Despite this success, there are challenges in scaling OGI-based LDAR to achieve rapid emission detection across vast geographic and temporal scales.

OGI surveys require an operator to manually inspect every potential leak source. Existing LDAR requirements typically specify one to four OGI surveys per year. The efficacy of these programs is limited by the probability that large unintended emissions (referred to as fugitive emissions or leaks) will persist for many months before detection. Ensuring that large emitters are quickly found and addressed therefore requires frequent LDAR surveys. However, frequent OGI-based LDAR surveys across thousands of sites quickly become logistically challenging and cost prohibitive.

Recently, several companies have developed novel approaches to methane leak detection that address the survey frequency limitation of OGI surveys [19]. Based on publicly available information, we can define three broad classes of new detection methods:

1. *Novel component or equipment-level survey methods:* OGI and EPA Method 21 surveys inspect every component and identify the source of emissions as part of the inspection. Drone- and some truck- and plane-based platforms provide similar specificity at

87   potentially higher survey speed and lower cost. Technologies in this class were tested
88   during the Stanford/EDF mobile monitoring challenge [19].
89   2. *Site level screening methods:* Rapid site-level screening may be used to identify high
90   emitting sites that warrant component-level secondary follow up surveys. Site-level
91   screening techniques were also tested in the mobile monitoring challenge and deployed in
92   numerous academic studies [19], [20].
93   3. *Continuous monitoring methods:* Sensors are permanently installed in proximity to oil
94   and gas sites and trigger follow up surveys when they detect an anomalous emission.
95   Like site-level screening programs, continuous monitors allow rapid detection of large
96   emissions while reducing the number of components that must be inspected directly.
97

98 Regulators and operators require a method for comparing the emissions reduction effectiveness
99 of LDAR programs using continuous monitoring and site- or equipment-level screening methods
100 to that of conventional LDAR programs. For example, Colorado's methane regulations require
101 periodic leak detection surveys using a handheld OGI camera or an equivalent technique [21].
102 However, the method for determining whether a technique is *equivalent* is not specified. This is
103 referred to as 'technology equivalence'.
104

105 A recent framework on technology equivalence developed jointly by scientists, industry experts,
106 and regulators emphasizes the role of models in comparing the performance of different
107 technologies and methods [22]. These models help evaluate new LDAR programs without the
108 need for expensive, time-consuming, and concurrent field-trials with new technologies.
109

110 In this work, we explore the equivalence of novel LDAR programs to conventional OGI-based
111 LDAR programs, demonstrate a model-based equivalence analysis, and provide
112 recommendations for cost-effective emissions mitigation policies. We examine the trade-offs in
113 survey speed, spatial resolution, and emissions mitigation between site-level and component-
114 level surveys using the Fugitive Emissions Abatement Simulation Toolkit (FEAST) [23]. FEAST
115 represents dynamic emissions from a gas field through time and models the emissions mitigation
116 resulting from LDAR programs. The results demonstrate that a higher frequency site level
117 screening survey coupled with a component level survey for repair may result in greater emission
118 reductions than a lower frequency component level survey without increasing costs. Critically,
119 we show that there is no one-size-fits-all approach to technology choice: emissions mitigation is
120 strongly affected by survey frequency, leak occurrence rates, and emissions size distribution. Our
121 approach illustrates how FEAST can provide the modelling framework required to evaluate
122 equivalency between disparate LDAR programs [22]. All model code and associated
123 documentation is made publicly available as part of this publication for use by scientists,
124 operators, and regulatory agencies.
125

126 ## 2   Methods
127 FEAST combines a stochastic model of methane emissions at upstream oil and gas facilities with
128 a model of leak detection and repair (LDAR) programs to estimate the efficacy and cost of
129 LDAR programs [23]. All simulation settings used in this work are further documented in the
130 supporting information (SI sections S2 and S3). A detailed description of the underlying model
131 construction can be found in [24].

2.1 Facility Descriptions – Activity Factors

Effective representation of methane emissions from upstream facilities requires both activity factors and emission characteristics corresponding to specific oil and gas basins. In this work, we use publicly available data from the U.S. EPA Greenhouse Gas Reporting Program (GHGRP) and the Colorado Oil and Gas Conservation Commission (COGCC) to create an activity model representative of sites in the Denver-Julesburg (DJ) basin [24-25]. On average, there are 1.9 wells per site in the DJ-basin, with a range between 1 and 51 wells per site. Activity data for this work also include component counts and frequency of unloading events (SI section S2).

2.2 Emissions Descriptions – Emissions Factors

FEAST simulates vents and fugitive emissions. Vents are emissions that occur by design, such as emissions from gas-driven pneumatic devices, and pressure-release valves. We also model liquid unloading events. For this work, unloading events are represented based on the total number of events and emissions reported to the GHGRP [25], while all other vents are approximated by drawing emission rates from an empirical distribution of observed emissions.

The fugitive emission model is characterized by an empirical emissions distribution and a leak production rate. FEAST simulates new leaks as independent random events in a Poisson process. The leak production rate is estimated based on the number of emissions found in repeated surveys of production equipment including tanks, pneumatics, and fugitive equipment under Colorado's OGI survey regulations [16], [27]. The empirical emission dataset is compiled from component level emission measurements from five recent publicly available studies [18], [28]–[31]. The studies included here did not distinguish between vents and leaks. In this work we assume that 46% of emissions simulated from the dataset are vents (see SI section S4.4 for additional detail). LDAR programs do not affect vented emissions in the simulation, but vents can cause site level surveys to trigger follow up actions at sites without significant fugitive emissions. The emission rate for each emission is drawn with replacement from the dataset. This approach is preferred compared to standard EPA emission factors approach because of the importance of super-emitters and skewed emissions distributions on the mitigation outcomes of LDAR programs. Additional information describing the data is available in SI section S2.

Several prior studies have demonstrated the highly skewed nature of methane emissions, with the top 5% of sites contributing to between 20% and 70% of total emissions depending on the geologic basin surveyed [35]–[38]. In a sensitivity analysis, we use a parametric emission size distribution to vary the contribution of the largest emitters to total emissions to understand how variability between basins will affect mitigation outcomes. The parametric distribution was defined such that emissions from the 80th percentile and larger were drawn from a power law distribution rather than the empirical distribution. The exponent characterizing the power law was then adjusted to achieve a range of skews in the emissions distribution as observed in field campaigns throughout North America. The parameterization maintains the median emission rate while exploring the range of equivalency conditions under different emission distributions.

2.3. Model Simulation:

Every FEAST run simulates undirected inspection and maintenance (UDIM) activities in addition to LDAR programs.. The UDIM model represents typical maintenance activities undertaken by operators. The UDIM model causes the total number of emissions to equilibrate

178 over time in the absence of an LDAR program as UDIM repairs offset the occurrence of new
179 fugitive emissions. The LDAR models simulate regulatory LDAR surveys that occur in addition
180 to UDIM activities. Comparing emissions in a UDIM-only scenario to an LDAR program helps
181 calibrate the model by comparing model derived emissions reduction from OGI-based LDAR
182 surveys to recent field data and regulatory models [18], [21]. The sensitivity of results to
183 variations in the assumed UDIM repair rate are explored in SI section S4.
184
185 2.4. LDAR Programs:
186 In this study, we simulate two types of LDAR programs: component-level detection programs
187 and tiered detection programs. Component level detection programs evaluate every component
188 for emissions independently and identify the source of emissions at the time of detection. Tiered
189 detection methods take a hybrid approach to leak detection: an initial survey to perform site-level
190 screening, followed by a second component-level survey to identify components for repair at
191 high-emitting sites.
192
193 2.4.1. Component-level survey:
194 OGI camera surveys are an example of a component level survey. Different component level
195 survey methods are distinguished by their probability of detection (PoD) curves, survey speed,
196 and cost as shown in Table 1. The median detection limit is defined as the leak size at which the
197 probability of detection is 50%. Several recent empirical, peer-reviewed performance assessment
198 studies are used to parameterize and validate the PoD curves [19], [27], [32]. Leaks detected by a
199 component level survey are immediately passed to the repair process which eliminates the leak
200 one day later.
201
202 2.4.2. Tiered surveys:
203 Tiered detection programs use a screening method to identify production sites with high
204 emission rates, similar to several existing plane-based technologies [20]. Like the component-
205 level detection model, the probability of detection curve is modeled as a sigmoid based on
206 empirical observations in recent peer-reviewed studies (SI section S3) [19]. For these
207 simulations, all sites with emissions that are detected by the screening method are flagged for
208 follow up by an OGI camera inspection to identify the source(s) of the emissions. Table 1 shows
209 the key parameters used in the OGI-based (component-level) and plane-based (tiered) LDAR
210 programs.
211
212 *Table 1 Key parameters used to specify detection methods.*

	Median detection limit (kg/day)	Survey speed	Cost ($/site)
OGI	2	6 sites/day	600 $/site
Plane	94	222 sites/day	100 $/site

213
214
215
216 2.3   Simulation settings
217 Simulations represent emissions from 100 well-sites over three years. The simulations have a
218 time resolution of one hour and 300 Monte Carlo iterations were completed for every LDAR
219 program and emission scenario represented in this work.

3   Results

The concept of technology equivalence is central to incorporating new technologies in regulatory LDAR programs [22]. While definitions vary across jurisdictions, it is typically defined in terms of mitigation outcomes – if two leak detection methods under separate LDAR program parameters achieve similar emissions mitigation, they are said to be equivalent. **We present a series of results that evaluate equivalency between LDAR programs with increasing degrees of freedom and implications for the cost-effectiveness of methane mitigation.**

3.1   Emission mitigation under OGI and tiered LDAR programs

Figure 1 shows the result of FEAST simulations for an upstream O&G basin with 100 well-sites under three different LDAR scenarios – UDIM, OGI survey, and a tiered program. The tiered program consists of an aerial screening survey with OGI follow up referred to as Plane + OGI. All surveys represented in Figure 1 are conducted semi-annually. The first of the two surveys start on day one in these simulations.

Figure 1.A shows the first 30 days of emissions during a single Monte Carlo iteration of FEAST for UDIM, OGI and Plane + OGI scenarios. Since LDAR programs only affect leaks, vented emissions are identical across all three scenarios. Unloading events result in the short duration spikes that drive the emission rate to over 20 kg/day per well. Figure 1.A shows that the rapid survey speed of the tiered detection method allows emissions to be found more quickly than a traditional OGI survey. However, the OGI method surpasses the Plane + OGI program by the end of the thirty-day period due to the lower detection threshold of the OGI survey in comparison to the preliminary aerial survey.

Figure 1.B extends the time series from Figure 1.A over the full three-year duration of the simulation. The time series shows the daily average emission rates. With a higher detection threshold than the OGI camera, the plane-based survey identifies fewer sites with emissions compared to OGI. Thus, fewer sites are flagged for follow up repair, resulting in higher average emissions when the two methods have the same survey frequency.

Figure 1.C shows the emissions mitigation achieved under both LDAR programs, relative to emissions in the UDIM scenario. A semi-annual OGI-based LDAR survey results in fugitive emissions mitigation of approximately 60%, similar to EPA's assumptions in its methane regulations [33]. By comparison, the Plane + OGI LDAR program achieves emissions mitigation of about 33% less than the conventional OGI survey. In this scenario, the two LDAR programs are not equivalent. The error bars represent variability from 300 Monte-Carlo iterations of the LDAR programs. Although FEAST models detection as a probabilistic process, the uncertainty range shown in Figure 1.C is driven by variability in the emission simulation rather than the detection simulation (See SI Figure S9). Therefore, the *relative* performance of the two simulated LDAR programs to each other is more certain than the *absolute* emissions in either case.

Figure 1.D shows the range of mitigation costs incurred by the OGI and Plane + OGI programs across the same 300 Monte Carlo iterations as Figure 1.C. Although the Plane + OGI program achieves less mitigation than the conventional OGI program, it does achieve a lower cost per ton of avoided CO_2 equivalent emissions. The mitigation cost for the Plane + OGI program is \$11/t

266 CO2e, about 31% lower than the $16/t CO2e cost for OGI-based mitigation. In this example, the
267 Plane survey flagged just 10% of sites for follow up surveys.

268
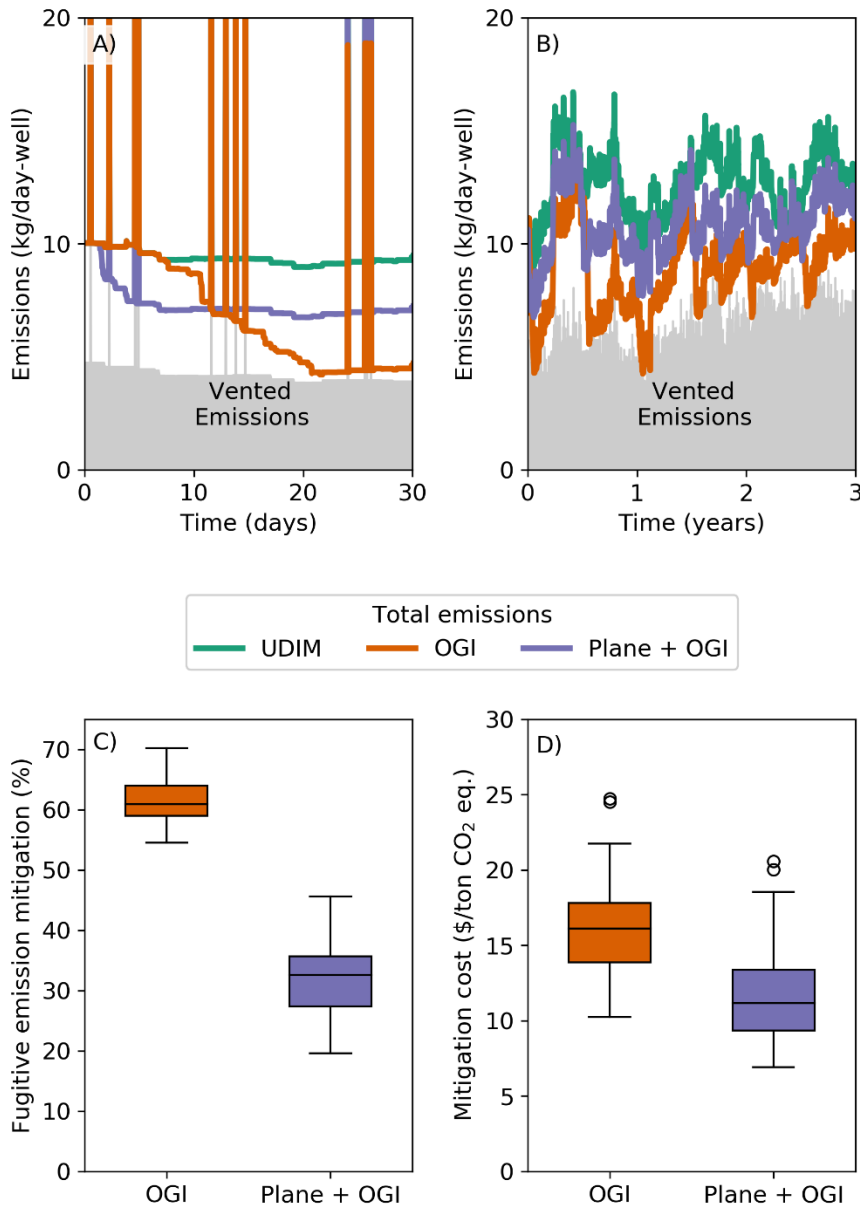
Figure 1. Results of FEAST simulations representing OGI surveys ("OGI") and plane-based screening
with OGI follow up ("Plane + OGI") at high emitting sites A.) 30 days of hourly emissions in a single
realization generated by FEAST B.) One-day moving average emission rate from a single realization
under three LDAR scenarios over the entire simulation period of 3 years C.) Distribution of mitigation
achieved by OGI and Plane+OGI LDAR programs D.) Distribution of mitigation costs for the OGI and
Plane+OGI LDAR programs. Outliers are greater than the 75th percentile by more than 1.5 times the
interquartile range.

276 **3.2 Mitigation equivalence dependence on survey frequency**
277 Since a plane-based survey will not detect as many emissions as an OGI survey, the Plane + OGI
278 program must survey more frequently to achieve equivalent emissions. Figure 2 shows the
279 impact of survey frequency on the mitigation and cost of the two LDAR programs.
280
281 Figure 2.A compares the component level and site level emission rate distributions under UDIM
282 conditions to the median detection thresholds of the OGI and Plane technology (see SI Figure S2
283 for additional details of the PoD curve). Overall, 94% of emissions come from sources larger
284 than the median detection threshold of the OGI camera. However, only 41% of emissions come
285 from sites with a total emission rate greater than the median detection limit of the Plane
286 technology.
287
288 Figure 2.B shows the emissions mitigation achieved through both LDAR programs as a function
289 of survey frequency. For the conventional OGI-based survey, increasing survey frequency from
290 two to four times per year increases mitigation from 60% to 73%. This is similar to the emissions
291 mitigation expected in federal regulations, where semi-annual and quarterly surveys reduce
292 emissions by 60% and 80%, respectively [33]. Thus, the model parameters here reproduce the
293 emissions mitigation current regulations expect to be achieved under different OGI-based LDAR
294 survey frequencies.
295
296 Increasing survey frequency reduces the duration of fugitive emissions. In the UDIM scenario,
297 leaks have an average duration of 208 days. Under an LDAR program, leaks that are large
298 enough to be detected will have an average duration of approximately one-half the time between
299 surveys: for example, quarterly surveys result in an average duration of approximately 45 days
300 for large leaks. LDAR programs mitigate emissions by reducing their duration.
301
302 Consider a mitigation target of 40% reduction in fugitive emissions. The conventional OGI-
303 based LDAR survey can achieve this mitigation target with an annual survey. Equivalently, the
304 tiered Plane + OGI LDAR program achieves 40% mitigation if the survey frequency is increased
305 to approximately 3 surveys per year. Higher levels of mitigation can be achieved with either
306 program if the survey frequency is increased further, although the plane-based survey cannot
307 achieve 80% mitigation even with monthly surveys due. While increasing the survey frequency
308 decreases the duration of detected emissions, emissions much smaller than the detection
309 threshold remain unaffected even at high survey frequencies. The detection threshold of a
310 screening technology thus places an effective upper bound on the amount of mitigation that can
311 be achieved.
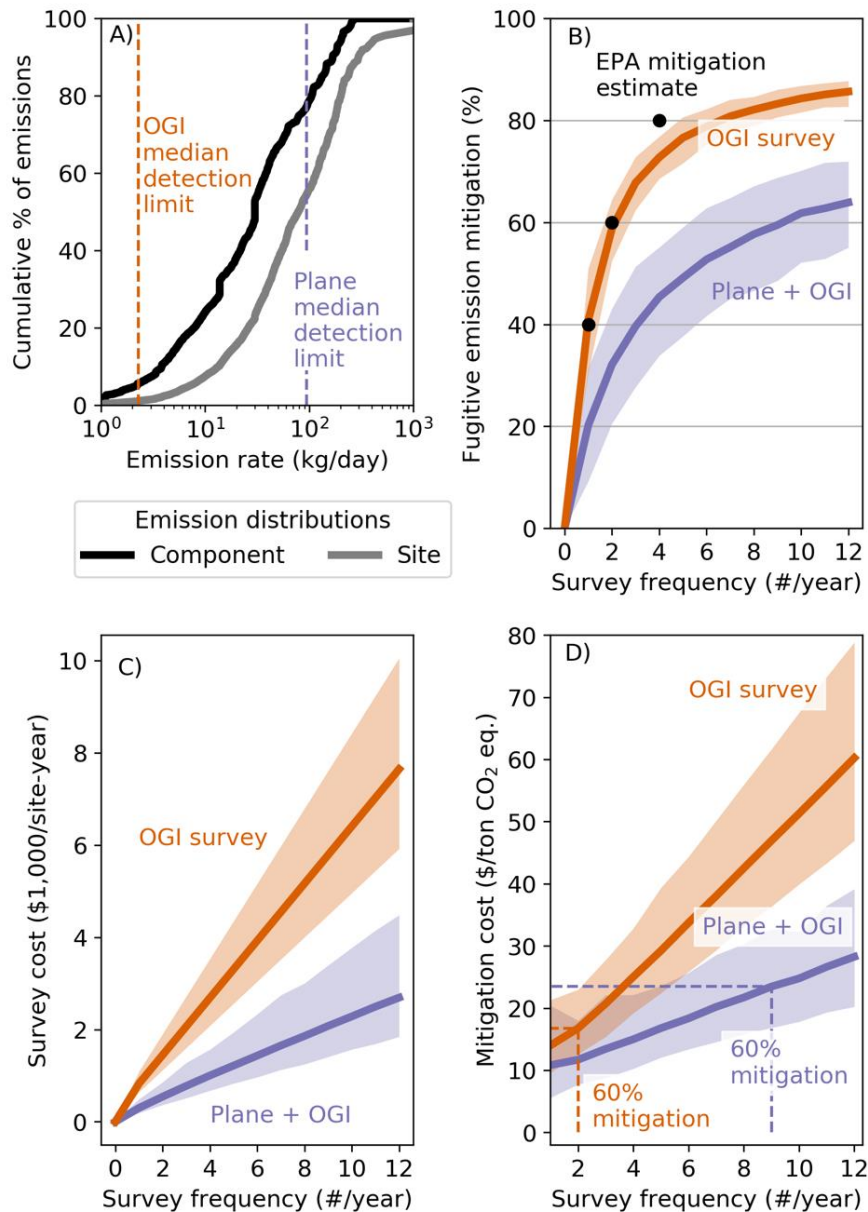
Figure 2. LDAR simulation results for an OGI detection threshold of 2 kg/day and a plane detection threshold of 94 kg/day A.) Component-level and site-level cumulative emission distributions with probability of detection curves for the simulated Plane and OGI detection methods. A-C) Fugitive emissions mitigation, survey cost and mitigation cost with OGI and Plane + OGI LDAR programs over a range of survey frequencies. Uncertainty ranges represent the 95% confidence interval generated by Monte Carlo iterations.

Figure 2.C shows that the cost of surveys for each LDAR program is proportional to the survey frequency. Prior studies have shown that the majority of costs associated with implementation of LDAR programs are reflected in the survey costs [34]. The US EPA's own analysis of its methane regulations show that semi-annual OGI-based LDAR surveys contributes to over 70% of the total cost of the LDAR program. The simulations shown in Figure 2.B-C suggest 60% fugitive emission reduction using either semi-annual OGI surveys or 9 plane-based screening surveys per year with OGI follow up. Under our cost assumptions, semi-annual OGI surveys

326 incur costs of $1400/site-year compared to $2000/site-year to achieve equivalent mitigation with
327 more frequent Plane + OGI surveys.
328
329 The results of Figure 2.B and 2.C were combined to generate Figure 2.D: the cost per metric ton
330 of CO_2 equivalent emissions mitigated. The nonlinear mitigation curve of Figure 2.B causes the
331 mitigation cost to increase more slowly for survey frequencies less than 3/year: as survey
332 frequency increases from zero, mitigation also increases partially offsetting the added survey
333 costs. At higher survey frequencies, mitigation approaches its asymptote resulting in near linear
334 growth in mitigation cost. The result illustrates that the marginal cost of mitigation increases as
335 the survey frequency increases.
336
337 ### 3.3   Cost-effectiveness of equivalent LDAR programs requires optimization across survey
338   frequency and detection threshold.
339 The cost-effectiveness of emissions mitigation depends on both the leak detection method and
340 the survey frequency. Here, we explore the cost-effectiveness of fugitive emissions mitigation
341 ($/t CO_2e) by modeling two generic leak detection methods – component-level surveys at an
342 average cost of $600/site and site-level surveys at $100/site. Follow up OGI surveys are charged
343 at the same rate per component as the generic component-level surveys. While keeping these
344 cost assumptions constant, Figure 3 illustrates how the mitigation cost changes depending on the
345 detection threshold and survey frequency of LDAR programs.
346
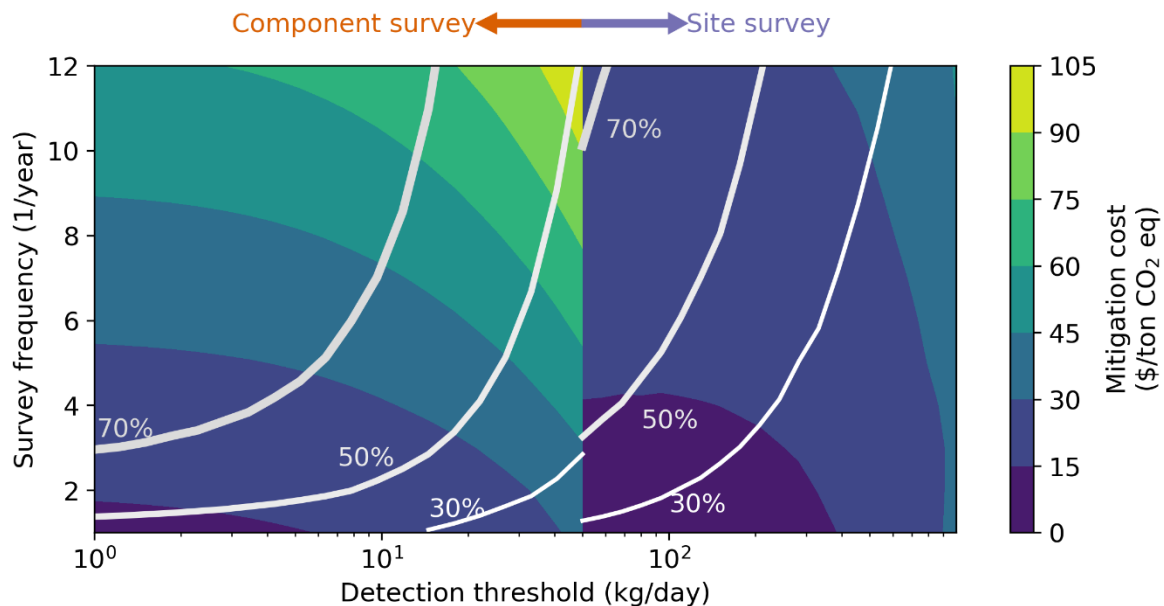
348 *Figure 3. CO_2 equivalent mitigation cost of modeled technologies over a range of survey frequencies and*
349 *detection thresholds. White contour lines indicate fugitive emissions mitigation percentages with the line*
350 *thickness proportional to mitigation level, while the color map indicates mitigation cost.*

351 Methods with detection thresholds above 50 kg/day were modeled as tiered detection programs
352 while methods with detection thresholds less than 50 kg/day were modeled as component-level
353 surveys. Constant-mitigation contours are indicated by white curves. For example, the curves
354 labeled 70% indicate all combinations of detection sensitivity and survey frequency that result in
355 70% mitigation of fugitive emissions. The location with the lowest cost along a mitigation

356   contour indicates the cost-optimal mitigation strategy for a particular mitigation target under
357   these assumptions.

358

359   Horizontal transects across the mitigation contours reveal the impact of increasing detection
360   threshold while holding the survey frequency constant. For small detection thresholds between 1
361   kg/d and 10 kg/d (high sensitivity), there is little change in mitigation as sensitivity increases
362   because small emitters account for a small fraction of total emissions. However, as the detection
363   threshold exceeds 10 kg/d, mitigation is more sensitive to detection threshold. Thus, while
364   increasing sensitivity of detection technology can improve mitigation outcomes, the marginal
365   improvement in sensitivity below about 10 kg/d does not result in a corresponding increase in
366   emissions mitigation. One can therefore trade high sensitivity for lower cost without adverse
367   mitigation outcomes.

368

369   Considering the color map of Figure 3 reveals trends in mitigation *cost*. Continuing with the
370   example site level detection threshold of 94 kg/day, the mitigation cost is 11 $/t CO_2e for a
371   survey frequency of 2/year but increases to 22 $/t CO_2e for a survey frequency of 8/year. In
372   addition, mitigation cost increases as detection threshold increases. This trend occurs because the
373   cost per component or site surveyed is independent of sensitivity in this simulation. The survey
374   cost of the component-level programs *remains constant* while the total mitigation *decreases*,
375   resulting in an overall *increase* in mitigation cost. By contrast, the costs of the tiered programs
376   *decline* as the detection threshold *increases* because fewer sites are flagged for follow up
377   surveys. However, the results show that the decrease in cost due to follow up surveys is not
378   sufficient to offset the decline in mitigation caused by increasing the detection threshold.

379

380   Tiered detection programs must efficiently direct ground crews to achieve sufficient emissions
381   mitigation without incurring secondary survey costs that exceed the savings achieved by the site
382   level survey. Tiered methods that identify high emitting *equipment* rather than *sites* may be more
383   successful if they can significantly reduce the time on site required of ground crews and avoid
384   misallocating ground crews due to vented emissions.

385

386   Our results also show that tiered detection programs are more cost effective if the mitigation goal
387   is less stringent. For example, Figure 3 shows tiered methods with a site level detection threshold
388   up to 300 kg/day can achieve 30% mitigation with less than 4 surveys per year more cost
389   effectively than annual component level surveys but are less competitive if the mitigation target
390   is increased to 70%. Similarly, a site-level technology with a detection threshold of 60 kg/d can
391   achieve 50% mitigation with quarterly surveys at a cost of $15/tCO2e, lower than the equivalent
392   semi-annual OGI-based LDAR survey cost of $ 17/tCO2e. The results from Figure 3 are
393   sensitive to the underlying emission rate distribution as described in the following section.

394

395   3.4   "Equivalence" depends on the natural gas basin where a technology is applied.
396   The skew of an emission distribution affects equivalence between LDAR programs. An LDAR
397   program that specializes in quickly identifying large leaks will perform better if emission
398   distributions are more skewed, because high-emitting sites will account for a greater fraction of
399   total emissions. Conversely, a component level method that surveys less frequently but has a
400   more sensitive detector will achieve a better mitigation fraction in less skewed distributions
401   because it will not allow midsize leaks to persist indefinitely. While Figures 1-3 rely on the

402   empirical emission distribution compiled for this work, this section explores how equivalence is
403   sensitive to changes in the emission distribution.
404
405   Figure 4 shows the technology detection threshold required to achieve a target emissions
406   mitigation level across different emission distributions. The orange and purple curves represent
407   mitigation under component level and tiered detection programs, respectively. In all cases, the
408   survey frequency was set to 6 surveys per year, while detection threshold was varied to achieve
409   the target emission mitigation rate.
410
411   In a highly skewed emission distribution as observed in the Uintah or Marcellus basin, 50%
412   mitigation can be achieved with a tiered detection program that has a detection threshold of 200
413   kg/day. However, a detection threshold of 50 kg/day would be required to achieve the same level
414   of mitigation in a less skewed distribution as observed in Medicine Hat in Alberta. More skewed
415   distributions allow the same mitigation targets to be achieved with a higher detection threshold,
416   resulting in a positive slope for all tiered and component surveys modeled in Figure 4.
417
418   The vertical gray lines show results from empirical studies conducted in the last five years from
419   U.S. and Canadian shale basins. Due to the sample size in these studies, the uncertainty in the
420   fraction of emissions from the top 5% of emitters may be large compared to the variability
421   between basins. The range of skew measured in various basins shown in Figure 4 give an
422   indication of the *combined* uncertainty and variability that exists in emission distributions.
423   Furthermore, the distribution of emissions that occur in a particular basin may evolve over time
424   due to maturing infrastructure, new wells, and production decline. An alternative LDAR program
425   may become more or less effective in comparison to OGI over time.
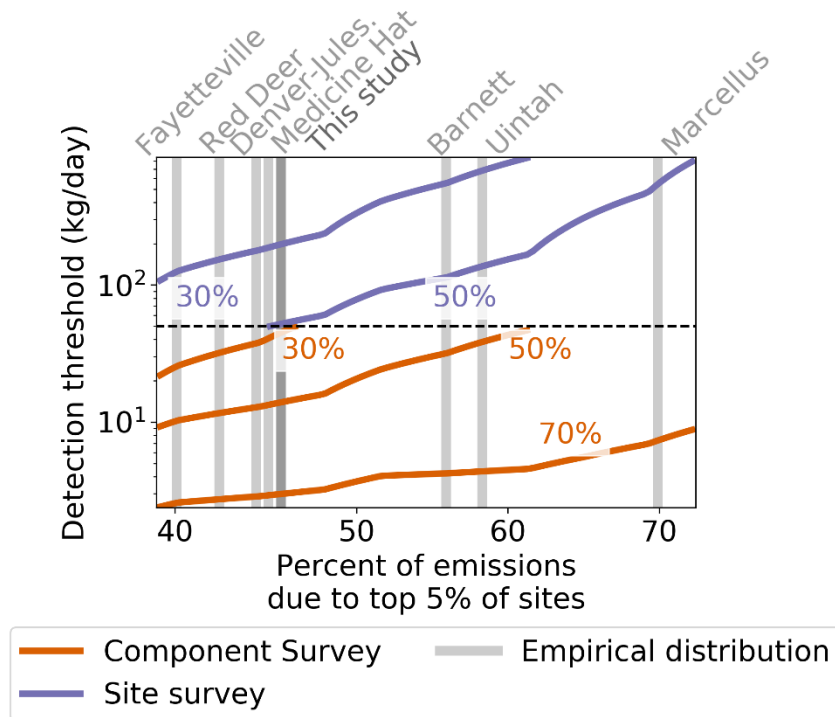
426
427   *Figure 4. The effect of emission size distribution on the detection threshold required to achieve a given*
428   *mitigation target. Purple and orange curves indicate the detection threshold required to achieve mitigation*
429   *for component and site level surveys, respectively. Follow up survey sensitivity is kept constant for all site*

430   *survey methods. Grey bars indicate the emission distribution skew observed in eight empirical studies of*
431   *site level emissions.*

4   Discussion and Study Limitations

433   According to the EPA greenhouse gas inventory, more than 5 million tons of methane leaked
434   from US natural gas infrastructure in 2018 [1]. New mobile and fixed-sensor technologies could
435   provide a cost-effective approach to reduce emissions. Yet, regulatory approval of these new
436   methods critically depends on a demonstration of equivalence to existing LDAR approaches. The
437   equivalence analysis described here provides the modeling framework required to quantitatively
438   compare LDAR programs while also highlighting the sensitivity of results to the underlying
439   emission model.

441   Equivalent emissions mitigation can be achieved with a broad range of sensitivities by choosing
442   the appropriate survey frequency and/or using a tiered detection approach. Tiered detection
443   approaches take advantage of the heavy-tailed nature of emission distributions to allocate
444   resources to the largest emissions, while component level surveys invest the same amount of
445   time in identifying emitters of all sizes. Tiered approaches must be efficient in dispatching
446   ground crews to offset the additional costs from increased survey frequencies.

448   Depending on their approach, LDAR programs will be affected differently by the emission size
449   distribution. While the composite emission distribution used in this work falls within the range of
450   emission distributions that exist in the US, Figure 4 shows that no distribution can accurately
451   represent all basins. Furthermore, the uncertainty in the tail of the component-level emission
452   distribution remains an important source of uncertainty in mitigation modeling. Accurately
453   representing mitigation requires improved measurements of emission distributions.

455   The "leak production rate" also remains a critical source of uncertainty in mitigation modeling.
456   While many studies have captured "snap shots" of the state of emissions in gas fields, much less
457   work has been done to repeatedly survey the same sites and evaluate the rate at which new
458   emissions occur. To separately evaluate the mean time to failure and the effect of undirected
459   maintenance activities, the same sites must be surveyed frequently, and emitters must be tracked
460   through time.

462   Additional empirical data would increase the confidence in equivalence assessments. The
463   sensitivity analysis presented in SI section S4 suggests that improving precision in the leak
464   production rate estimate will decrease uncertainty the most, followed by developing basin-
465   specific emission distributions. Coupling FEAST with a process-based model similar to that
466   described by Cardoso-Saldon et al. [39] would provide a more accurate model of vents and
467   further reduce uncertainty.

469   We draw the following broad conclusions from the results of this work that can aid oil and gas
470   operators and regulatory agencies in developing LDAR programs using new methane detection
471   technologies:
472   1. Equivalent emissions mitigation can be achieved by LDAR programs with different
473   detection thresholds by varying the survey frequency.

475   2. Median detection threshold of new technologies, to first order, present effective lower
476   and upper bounds for emissions mitigation. At the lower end, decreasing the detection
477   threshold below 10 kg/d does not increase mitigation outcomes proportionally because of
478   skewed leak-size distributions. At the upper end, emissions mitigation with high median
479   detection threshold technologies does not increase in proportion to survey frequency as
480   emissions smaller than the detection threshold remain unaffected even at high survey
481   frequencies.
482
483   3. Vented emissions play a critical role in the cost-effectiveness of tiered detection
484   programs that direct ground crews based on site-level emissions detection. Without a
485   reliable way to differentiate sites with high vented emissions from those with high
486   fugitive emissions, tiered programs risk directing ground crews to many sites with little
487   mitigation benefit, thereby increasing costs.
488
489   4. The survey frequency and detection threshold required for equivalent emission mitigation
490   will depend on the emission size distribution in the basin where the LDAR program is
491   applied. Evaluation of the efficacy of LDAR programs and technology equivalence
492   periodically to account for (a) changes to emission-size distribution, and (b) reduction in
493   emissions over time will be critical to ensure mitigation targets are achieved throughout
494   the duration of the program.
495
496   New methane detection technologies and platforms – continuous and survey-based – represent an
497   opportunity to cost-effectively address methane emissions from the oil and gas industry. The
498   degrees of freedom in LDAR program parameters such as technology choice, hybrid detection,
499   survey frequency, and detection threshold provide a method to design methane mitigation
500   policies that best tackle issues specific to the gas field or operator. As states and countries around
501   the world converge on methane emissions as a cost-effective, near-term approach to address
502   climate change, FEAST is a quantitative tool to for assessing new technologies, evaluating the
503   outcomes of mitigation programs, and achieving methane mitigation targets. Future work on this
504   model will seek to enable the evaluation of satellite technologies and continuous monitoring
505   systems to provide a near real-time monitoring of methane emissions across the world. In light of
506   the potential use of this model in regulatory rule making, all model code and documentation are
507   made publicly available as part of this publication, including any future updates.
508
509
516
517
518
519
520

521   References:
522
523   [1]   U.S. Environmental Protection Agency, "Inventory of U.S. Greenhouse Gas Emissions
524   and Sinks: 1990-2018 – EPA 430-R-20-002," Apr. 2020. Accessed: Aug. 13, 2020.
525   [Online]. Available: https://www.epa.gov/ghgemissions/inventory-us-greenhouse-gas-
526   emissions-and-sinks.
527   [2]   G. Myhre *et al.*, "Chapter 8: Anthropogenic and Natural Radiative Forcing," in *Climate*
528   *Change 2013: The Physical Science Basis. Contribution of Working Group I to the Fifth*
529   *Assessment Report of the Intergovernmental Panel on Climate Change*, T. F. Stocker, D.
530   Qin, G.-K. Plattner, M. Tignor, S. K. Allen, J. Boschung, A. Nauels, Y. Xia, V. Bex, and
531   P. M. Midgley, Eds. Cambridge, United Kingdom and New York, NY, USA, 2013, pp.
532   659–740.
533   [3]   D. J. Zimmerle *et al.*, "Methane Emissions from the Natural Gas Transmission and
534   Storage System in the United States," *Environ. Sci. Technol*, vol. 49, p. 54, 2015, doi:
535   10.1021/acs.est.5b01669.
536   [4]   R. A. Alvarez *et al.*, "Assessment of methane emissions from the U.S. oil and gas supply
537   chain," *Science (80-.).*, 2018, doi: 10.1126/science.aar7204.
538   [5]   A. Brandt *et al.*, "Methane Leaks from North American Natural Gas Systems," *Science*
539   *(80-.).*, vol. 343, pp. 733–735, 2014.
540   [6]   R. W. Howarth, "Ideas and perspectives: is shale gas a major driver of recent increase in
541   global atmospheric methane?," *Biogeosciences*, vol. 16, pp. 3033–3046, 2019, doi:
542   10.5194/bg-16-3033-2019.
543   [7]   I. A. G. Wilson and I. Staffell, "Rapid fuel switching from coal to natural gas through
544   effective carbon pricing," *Nat. Energy*, vol. 3, no. 5, pp. 365–372, May 2018, doi:
545   10.1038/s41560-018-0109-0.
546   [8]   K. Tanaka, O. Cavalett, W. J. Collins, and F. Cherubini, "Asserting the climate benefits of
547   the coal-to-gas shift across temporal and spatial scales," *Nat. Clim. Chang.*, vol. 9, no. 5,
548   pp. 389–396, 2019, doi: 10.1038/s41558-019-0457-1.
549   [9]   X. Zhang, N. P. Myhrvold, Z. Hausfather, and K. Caldeira, "Climate benefits of natural
550   gas as a bridge fuel and potential delay of near-zero energy systems," 2015, doi:
551   10.1016/j.apenergy.2015.10.016.
552   [10]   A. L. Rich and H. T. Orimoloye, "Elevated Atmospheric Levels of Benzene and Benzene-
553   Related Compounds from Unconventional Shale Extraction and Processing: Human
554   Health Concern for Residential Communities," *Environ. Health Insights*, vol. 10, pp. 75–
555   82, 2016, doi: 10.4137/EHI.S33314.
556   [11]   IPCC, *Global warming of 1.5°C An IPCC Special Report on the impacts of global*
557   *warming of 1.5°C above pre-industrial levels and related global greenhouse gas emission*
558   *pathways, in the context of strengthening the global response to the threat of climate*
559   *change,*. 2018.
560   [12]   D. Huppmann *et al.*, "IAMC 1.5°C Scenario Explorer and Data hosted by IIASA."
561   Integrated Assessment Modeling Consortium & International Institute for Applied
562   Systems Analysis, 2018, doi: 10.22022/SR15/08-2018.15429.
563   [13]   "Canada's methane regulations for the upstream oil and gas sector," *Government of*
564   *Canada*, 2018. https://www.canada.ca/en/environment-climate-change/services/canadian-
565   environmental-protection-act-registry/proposed-methane-regulations-additional-
566   information.html (accessed Aug. 13, 2019).

567 [14] C. Ruiz-Funes, *DISPOSICIONES ADMINISTRATIVAS DE CARÁCTER GENERAL QUE*
568 *ESTABLECEN LOS LINEAMIENTOS PARA LA PREVENCIN Y EL CONTROL*
569 *INTEGRAL DE LAS EMISIONES DE METANO DEL SECTOR HIDROCARBUROS*.
570 2018.

571 [15] "Final Regulation Order Subarticle 13: Greenhouse Gas Emission Standards for Crude Oil
572 and Natural Gas Facilities." California Code of Regulations, pp. 1–71, 2017.

573 [16] *Control of Ozone via Ozone Precursors and Control of Hydrocarbons via Oil and Gas*
574 *Emissions*. 2018.

575 [17] *Wyoming Administrative Rules Chapter Environmental Quality Dept. of Air Quality*
576 *Chapter 8: Nonattainment Area Regulations*. US, 2018.

577 [18] A. P. Ravikumar *et al.*, "Repeated leak detection and repair surveys reduce methane
578 emissions over scale of years," *Environ. Res. Lett.*, 2020, doi: 10.1088/1748-9326/ab6ae1.

579 [19] A. Ravikumar *et al.*, "Single-blind Inter-comparison of Methane Detection Technologies--
580 Results from the Stanford/EDF Mobile Monitoring Challenge," 2019, [Online]. Available:
581 https://doi.org/10.1525/elementa.373.

582 [20] T. A. Fox, T. E. Barchyn, D. Risk, A. P. Ravikumar, and C. H. Hugenholtz, "A review of
583 close-range and screening technologies for mitigating fugitive methane emissions in
584 upstream oil and gas," *Environ. Res. Lett.*, vol. 14, no. 5, p. 053002, Apr. 2019, doi:
585 10.1088/1748-9326/ab0cc3.

586 [21] *Control of Ozone via Ozone Precursors and Control of Hydrocarbons via Oil and Gas*
587 *Emissions*. 2019.

588 [22] T. A. Fox *et al.*, "A methane emissions reduction equivalence framework for alternative
589 leak detection and repair programs," *Elem Sci Anth*, 2019, doi: 10.1525/elementa.369.

590 [23] C. E. Kemp, A. P. Ravikumar, and A. R. Brandt, "Comparing Natural Gas Leakage
591 Detection Technologies Using an Open-Source 'virtual Gas Field' Simulator," *Environ.
592 Sci. Technol.*, vol. 50, no. 8, 2016, doi: 10.1021/acs.est.5b06068.

593 [24] C. E. Kemp, A. P. Ravikumar, and A. R. Brandt, "Comparing Natural Gas Leakage
594 Detection Technologies Using an Open-Source Virtual Gas Field Simulator," *Environ.
595 Sci. Technol*, 2016, doi: 10.1021/acs.est.5b06068.

596 [25] U.S. Environmental Protection Agency, "Facility Level Information on Greenhouse Gases
597 Tool," 2017. https://ghgdata.epa.gov/ghgp/main.do#/listFacilityForBasin/?q=Find a
598 Facility or Location&bs=540&fid=&sf=11001000&lowE=-
599 20000&highE=23000000&g1=1&g2=1&g3=1&g4=1&g5=1&g6=0&g7=1&g8=1&g9=1
600 &g10=1&g11=1&g12=1&s1=0&s2=0&s3=0&s4=0&s5=0&s6=0&s7=0&s8=0&s9=1&s1
601 0=0& (accessed Oct. 23, 2019).

602 [26] COGCC, "COGCC/Data Downloads/GIS/Well Surface Location Data (Updated
603 Daily)/Well Spots (APIs)," *Colorado Oil and Gas Conservation Commission*, 2019.
604 https://cogcc.state.co.us/documents/data/downloads/gis/WELLS_SHP.ZIP (accessed Jan.
605 13, 2020).

606 [27] A. P. Ravikumar, J. Wang, M. Mcguire, C. S. Bell, D. Zimmerle, and A. R. Brandt, "Good
607 versus Good Enough? Empirical Tests of Methane Leak Detection Sensitivity of a
608 Commercial Infrared Camera," *Environ. Sci. Technol*, vol. 52, 2018, doi:
609 10.1021/acs.est.7b04945.

610 [28] D. Allen *et al.*, "Measurements of methane emissions at natural gas production sites in the
611 United States David," *Proc. Natl. Acad. Sci.*, vol. 110, no. 44, pp. 18025–18030, Sep.
612 2013, doi: 10.1073/pnas.1315099110.

613 [29] "City of Fort Worth Natural Gas Air Quality Study," Fort Worth, TX, 2011. [Online].
614   Available: http://fortworthtexas.gov/uploadedFiles/Gas_Wells/AirQualityStudy_final.pdf.
615 [30] J. Kuo, "Final project report estimation of methane emissions from the California Energy
616   Commission," 2012. doi: 500-09-007.
617 [31] C. S. Bell *et al.*, "Comparison of methane emission estimates from multiple measurement
618   techniques at natural gas production pads," *Elem Sci Anth*, vol. 5, no. 0, p. 79, Dec. 2017,
619   doi: 10.1525/elementa.266.
620 [32] D. Zimmerle, T. Vaughn, C. Bell, K. Bennett, P. Deshmukh, and E. Thoma, "Detection
621   Limits of Optical Gas Imaging for Natural Gas Leak Detection in Realistic Controlled
622   Conditions," *Environ. Sci. Technol.*, vol. 54, no. 18, pp. 11506–11514, 2020, doi:
623   10.1021/acs.est.0c01285.
624 [33] "Oil and Natural Gas Sector : Standards for Crude Oil and Natural Gas Facilities:
625   Background Technical Support Document for the Proposed New Source Performance
626   Standards 40 CFR Part 60, subpart OOOOa." EPA, Chapel Hill, NC, 2016, [Online].
627   Available: https://beta.regulations.gov/document/EPA-HQ-OAR-2010-0505-7631.
628 [34] A. P. Ravikumar and A. R. Brandt, "Designing better methane mitigation policies: the
629   challenge of distributed small sources in the natural gas sector," *Environ. Res. Lett.*, vol.
630   23, no. 044023, 2017, doi: 10.1088/1748-9326/aa6791.
631 [35] A. M. Robertson *et al.*, "Variation in Methane Emission Rates from Well Pads in Four Oil
632   and Gas Basins with Contrasting Production Volumes and Compositions," 2017, doi:
633   10.1021/acs.est.7b00571.
634 [36] C. W. Rella, T. R. Tsai, C. G. Botkin, E. R. Crosson, and D. Steele, "Measuring Emissions
635   from Oil and Natural Gas Well Pads Using the Mobile Flux Plane Technique," *Environ.
636   Sci. Technol*, vol. 49, p. 4748, 2015, doi: 10.1021/acs.est.5b00099.
637 [37] M. Omara, M. R. Sullivan, X. Li, R. Subramanian, A. L. Robinson, and A. A. Presto,
638   "Methane Emissions from Conventional and Unconventional Natural Gas Production
639   Sites in the Marcellus Shale Basin," 2016, doi: 10.1021/acs.est.5b05503.
640 [38] E. O'Connell *et al.*, "Methane emissions from contrasting production regions within
641   Alberta, Canada: Implications under incoming federal methane regulations," *Elementa*,
642   vol. 7, no. 1, 2019, doi: 10.1525/elementa.341.
643 [39] F. J. Cardoso-Saldañ and D. T. Allen, "Projecting the Temporal Evolution of Methane
644   Emissions from Oil and Gas Production Sites," *Cite This Environ. Sci. Technol*, vol. 54,
645   pp. 14172–14181, 2020, doi: 10.1021/acs.est.0c03049.
646
647

New Technologies can Cost-effectively Reduce Oil and Gas Methane Emissions, but Policies will Require Careful Design to Establish Mitigation Equivalence

Chandler E. Kemp, and Arvind P. Ravikumar

Department of Systems Engineering, Harrisburg University of Science and Technology, Harrisburg PA 17101

Supplementary Information
23 pages, 9 figures, 4 tables

Contents

45
46

S1.   Introduction

48   The results presented in the main text rely on the Fugitive Emission Abatement Simulation
49   Toolkit (FEAST). Section S1 is this introduction. The parameters used to specify emissions and
50   LDAR programs in FEAST are further explained in sections S2 and S3, respectively. Section S4
51   presents a sensitivity analysis that describes how uncertainty in the input parameters impact
52   results.

S2.   Emissions Model

54
S2.1 Activity Data
56   FEAST represents production infrastructure as a hierarchy of components and sites. A simulation
57   contains many sites, and a site contains many components. Every component can be a source of
58   fugitive emissions, uncategorized vents, or unloading emissions.
59
60   Sites in this study are modeled after upstream well pads at unconventional oil and gas sites.
61   Given the modular nature of the site representation, detailed activity data (equipment per site,
62   components per equipment) can be used to represent any oil and gas facility, thereby expanding
63   the potential use for the model. Each site is assigned a fixed number of wells drawn with
64   replacement from the population of well pads in Colorado. The Colorado Oil and Gas
65   Conservation Commission (COGCC) releases production and location data for all gas wells in
66   their jurisdiction [1]. We grouped wells within 50 meters of a given well into sites to establish a
67   distribution of the number of wells per site following the method described by Omara et al. [2].
68   We then assumed that there were, on average, 650 components per well at each site. The
69   estimate includes all components at the site, rather than the components that are part of the
70   wellheads and is similar to the natural gas well site model plant developed by the EPA [3]. Every

71   Monte Carlo iteration of the model used in this work contained 100 sites, but the number of wells
72   at each site was chosen randomly for each iteration.
73
74   ## S2.2 Fugitive emissions and unclassified vents
75   Our simulation of fugitive emissions and unclassified vents is driven by publicly available data.
76   While numerous studies have measured emissions at the component level on well pads, few have
77   distinguished between vents and fugitive emissions. Here, we define vents as any emissions that
78   occur by design and will not be affected by an LDAR program. We define fugitive emissions as
79   emissions that are unintentional and can be stopped if detected.
80
81   While some emissions are simple to classify on site, others are prohibitively complex for typical
82   survey teams. For example, a pressure relief valve may be emitting when surveyors are on site
83   but determining whether that emission is a vent caused by a temporary high-pressure condition, a
84   leak caused by a faulty valve, or a leak caused by a faulty piece of equipment upstream of the
85   valve may be beyond the scope of the detection survey. Furthermore, not all operators and
86   surveyors use the same definition of a fugitive emission. For example, some jurisdictions classify
87   all tank related emissions as vents [4] while others distinguish between different types of tank
88   emissions [5].
89
90   Therefore, we designate 45% of emissions as vents. In practice, field students at oil and gas
91   facilities have found a wide variation in the fraction of emissions that can be classified as vents.
92   The effect of changing this percentage is examined in the sensitivity analysis in section S4.
93
94   ### S2.2.1 Emission rate distribution
95   We compiled a database of component-level emission surveys based on publicly available data
96   to populate the emissions model in FEAST. To be included in the database, the surveys were
97   required to meet the following three criteria:
98   1. The surveys were conducted at upstream production facilities,
99   2. The study included all emissions that could be measured at production facilities,
100   3. Emission rates were measured at the component level.
101 Criteria two excludes studies that focused on a particular component type. This restriction
102 allowed direct use of the emissions dataset to generate a distribution of fugitive emission rates
103 for well sites. Future work may use component-specific emission distributions and require
104 component-type activity data, but supporting that complexity is beyond the scope of this
105 analysis. Criteria two ensures that the emission data used are from the industry segment of
106 interest to this work. Criteria three is necessary because detection technologies that identify
107 emissions at the component level were modeled in this work. Furthermore, we can aggregate
108 component-level data to the equipment-level, while the reverse disaggregation is typically
109 impossible without information on emitting components.
110
111 Five major studies were identified that satisfy all three criteria as summarized in
112 . Comparing the studies in pairs using a two sample Kolmogorov-Smirnov test shows that each
113 study resulted in an independent emission distribution (all pair-wise p-values $\ll 0.01$). Several
114 factors contribute to the differences in the observed distributions. First, the studies took place in
115 disparate geologic basins, operating environments, and geographic locations. The five surveys
116 spanned sites in Alberta, California, Colorado, Arkansas, Texas, and Appalachia. The

117 characteristics of gas fields across these locations are very different. For example, most wells in
118 California are vertical with one well per pad, while most wells in Colorado are drilled
119 horizontally and well pads service multiple wells. Gas wells in Appalachia tend to produce dry
120 gas while the fields in Alberta produce gas and oil. The variety of drilling practices, resource
121 characteristics and infrastructure are expected to affect the size distribution of emissions.
122
123 Furthermore, the studies used distinct methods to identify emissions. Allen and Ravikumar used
124 optical gas imaging (OGI) technology to identify emissions. ERG identified some emissions
125 using an OGI camera and others with a Toxic Vapor Analyzer (TVA). The emission distributions
126 associated with each technology are shown separately in Figure S1. Bell used an OGI camera
127 and a Tunable Diode Laser Absorption Spectroscopy (TDLAS) technology to detect emissions.
128 Emissions from both methods are combined in one distribution because the emissions were not
129 segregated by detection method in the study. Kuo also used a TDLAS technology for detection.
130

131 *Table S1 Studies included in populating the empirical emission-size distributions in FEAST. Year*
132 *indicates the year when the study was published (not the year when measurements were made). The*
133 *number of sites refers to the number of well pad production sites included in the study. The number of*
134 *emissions identified includes both measured and unmeasured (non-quantified, but only detected)*
135 *emissions.*

Citation	Lead author	Year	Number of sites	Number of wells	Number of emissions identified	Survey method
[6]	Allen	2013	150	489	769	OGI
[7]	ERG	2011	375	1121	1193	OGI
[7]	ERG	2011		112	756	TVA
[8]	Kuo	2012		128	94	TDLAS
[9]	Bell	2017	261		322	OGI and TDLAS
[4]	Ravikumar	2020	27		1236	OGI

136
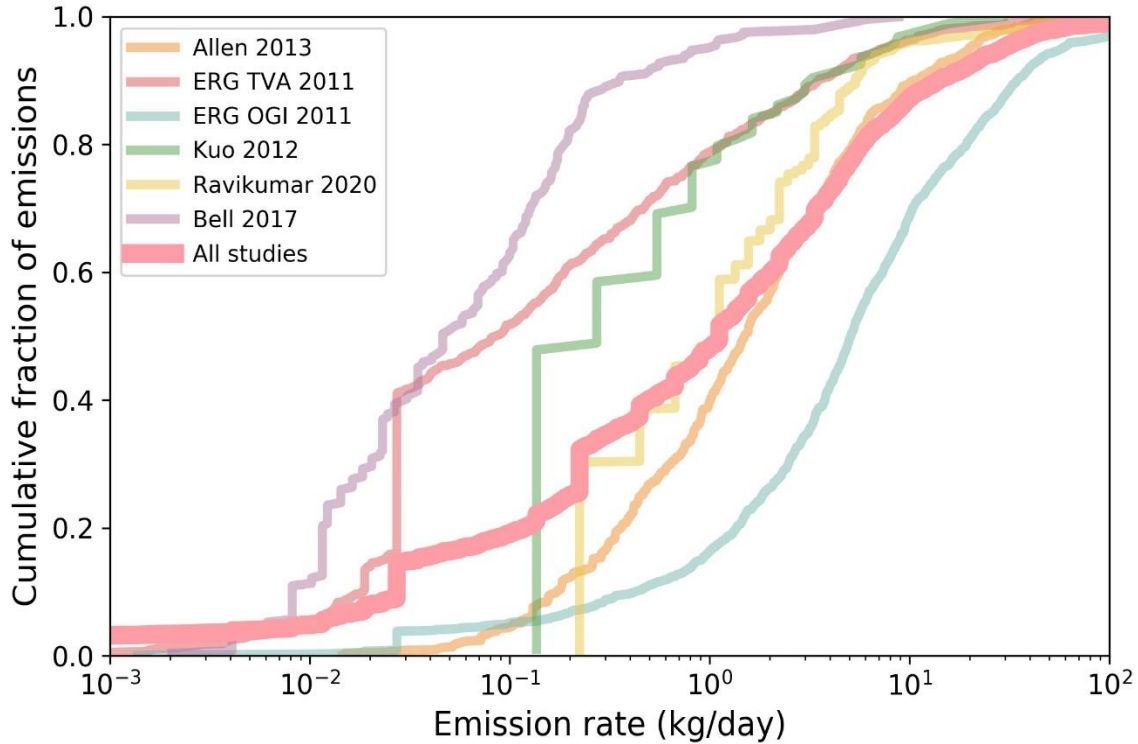
Figure S1 Component-level emission-size distribution measured in each of the studies summarized in Table S1.

S2.3 Pneumatic controllers

Pneumatic controllers have been estimated to contribute 23% and 27% of total natural gas emissions from the production sector [10], [11]. Since all studies in the emissions distribution database except Bell 2017 include pneumatic controller emissions, pneumatic controllers are treated as an unclassified vent in this work. As a result, the frequent short duration characteristics of pneumatic emissions are not captured by this model.

S2.3.1 Emission distribution sensitivity

The component-level emissions distribution has at least three sources of uncertainty:
1. Finite sample size
2. Potential for bias in measurements
3. Regional variability

The heavy tailed distribution of emission sizes and associated uncertainty has been broadly acknowledged [12]. The bootstrapping method used in this work to select emission sizes avoids biasing the data with a parametric model. However, the method is limited by the finite sample size and does not simulate any emissions larger than those captured in the empirical data.

There is also a bias introduced to our work because only emissions that were detected and measured can be included. In some cases, safety or access related challenges may have prevented important emissions from being quantified in field campaigns. For example, Ravikumar et al. reported that all tank emissions detected in their study were not directly quantified. Previous studies have shown that tank emissions are often a source of large emissions that account for

163 over one third of total emissions from production sites [4]. To overcome this bias, Ravikumar et
164 al. appended the emission data set with an estimate of tank emissions based on results from other
165 studies. By incorporating many component level emission studies using a variety of detection
166 methods, we aim to reduce the potential for systematic bias in the emission dataset. As more
167 component-level studies are made publicly available and incorporated in this model, the
168 empirical size distributions will become more representative of actual size distributions.
169
170 We explore the sensitivity of results to the emission rate distribution in the sensitivity analysis. In
171 addition to choosing emission rates from the empirical distribution using bootstrapping, we also
172 use a constrained power law distribution, as described below. The power law distribution allows
173 us to observe the impact of manipulating the large emission tail of the distribution.
174

175 ### S2.3.2 Bootstrap emission size selection
176 The skew of the emission size distribution is well documented and influences the efficacy of leak
177 detection programs [12]. Bootstrap sampling of emission rates from an empirical distribution is
178 the most robust method for representing heavy-tailed emission distributions [12]. In this work,
179 we used bootstrap sampling to generate results for Figures 1-3 in the main text and employed a
180 constrained power-law distribution in sensitivity analysis. Specifically, every emission generated
181 by FEAST is assigned an emission rate drawn randomly with replacement from the emission rate
182 database.
183

184 ### S2.3.3 Power law emission size selection
185 Power law emission distributions are useful for exploring the impact of emission distribution on
186 mitigation equivalence. The results shown in Figure 4 in the main text use power law emission
187 distributions. We generated the distributions using bootstrap sampling from the compiled
188 emission database up to the 80th percentile and a power law distribution of emission rates for
189 larger emissions. The probability density function for emission rates greater than the 80th
190 percentile is shown in Equation S1, where α is a tuning parameter and x is an emission rate. In
191 order to prevent impossible emission rates, the power law distribution was not allowed to exceed
192 the simulated gas production rate at the site where the emission occurred (Q_{site}). Q_{site} was
193 drawn from the distribution of production rates at sites in Colorado with the same number of
194 wells as the simulated site [1].

$$p(x|x > x_{80\%}) = \min\left(\frac{\alpha - 1}{x_{80\%}}\left(\frac{x}{x_{80\%}}\right)^{-\alpha}, \; Q_{site}\right) \qquad (S1)$$

195
196 The method described above allows direct manipulation of the tail of the empirical distribution
197 — to which tiered detection methods are particularly sensitive, and data are sparse — while
198 maintaining the median emission rate. In contrast, the tail of a lognormal distribution cannot be
199 tuned without also affecting the median emission rate and lognormal distributions have been
200 shown to under-estimate the tail of component-level emission distributions [12].
201
202 The expected number of emissions present during the undirected inspection and maintenance
203 (UDIM) scenario is determined based on the average emissions per well in the compiled
204 emission data set, equivalent to about 1.5 emissions per well. The number of components leaking
205 at the beginning of the simulation is determined by drawing from a binomial distribution with a

206   leak probability that results in an average of 1.5 emissions per well. The mean duration of
207   emissions in the UDIM scenario (T_{Emit}) is set according to Equation (S2, where N_e is the
208   expected number of emissions and N_c is the number of components. In an UDIM simulation, the
209   duration of every fugitive emission and unclassified vent is drawn from an exponential
210   distribution parameterized with T_{Emit}. Setting T_{Emit} according to Equation (S2 ensures that while
211   the number of emissions varies during and between simulations, the expectation value of the
212   number of emissions is consistent with emission rates observed in the field.

$$T_{Emit} = \frac{N_e}{N_c} T_{Failure}$$ (S2)

213
214

215   S2.4 Unloading events
216   Unloading emissions refer to gas that is vented in the process of removing accumulated liquids
217   from wells. While some wells require automated plunger lift systems and unload hundreds of
218   times per year, other wells only require a few unloading events per year and can be triggered
219   manually. The frequency of unloading events varies between geologic basins. This work
220   simulates production sites in the DJ basin, where unloading events are relatively rare.
221
222   Unloading emissions are unique because they are not included in the component-level surveys
223   used for the fugitive and uncategorized vent models. They are modeled explicitly in FEAST as it
224   can be a significant contributor to total methane emissions in liquids-rich basins. The unloading
225   model allows for three types of wells: wells that do not unload, wells that use plungers to remove
226   liquids, and wells that unload without a plunger. The parameters used to specify these emissions
227   are provided in Table S2. The number of events per year and the emissions per event are both set
228   to average values calculated using emission data from the EPA greenhouse gas reporting
229   program (GHGRP) for the DJ basin [13]. The duration of the events is set to the average value of
230   the duration distribution reported by Zaimes et al [14].
231
232   *Table S2 Unloading parameters in FEAST for wells with and without plunger lifts.*

	Plunger unloading	No plunger unloading
Average duration (minutes)	34	83
Average emission rate (kg/hr)	181	277
Frequency (#/year)	6	0.1

233

234   S2.4.1 Number of unloading wells
235   All facilities that emit more than 25,000 metric tons CO_2e greenhouse gases annually are
236   required to report to the GHGRP. In the case of onshore oil and gas production, a "facility" is
237   defined as all wells and associated production equipment in a geologic basin owned by a single
238   entity [15]. In 2017, 16 companies operating 23,037 wells in Colorado reported emissions.
239
240   The fraction of wells that reported plunger and no-plunger unloading events were used to
241   designate the number of unloading wells in the base case simulations. Specifically, the GHGRP
242   reported 2662 (11.6%) plunger-unloading wells and 541 (2.3%) no-plunger-unloading wells for
243   the state of Colorado.

244

S2.4.2 Emission profiles

246 To simulate LDAR programs, FEAST requires a duration and emission rate for every emission.
247 The GHGRP data provides the total emission from unloading events and the number of events by
248 facility for plunger and non-plunger wells separately. Therefore, the GHGRP data can be used to
249 calculate the average emission mass per event for plunger and non-plunger wells. The GHGRP
250 does not provide unloading emission data at the well level or event level, so a distribution of
251 emission sizes cannot be determined. The GHGRP does not provide the duration of events either,
252 so a flux rate cannot be directly estimated from the GHGRP data. Instead, the average emission
253 duration reported by Zaimes is used for all unloading events in the base case simulation, and the
254 flux rate is calculated based on the average emission volume and duration. Zaimes reports that 3
255 out of 2532 venting wells use automatic unloading systems in the DJ basin. Therefore, the
256 manual no-plunger (4974 seconds) and manual plunger (2059 seconds) durations are used.

257

S2.4.3 Unloading model uncertainties

259 All facilities in Colorado in 2017 estimated emissions using Method 2 or Method 3 specified in
260 40 CFR Subpart W § 98.233 based on the type of unloading (plunger or no-plunger), well
261 geometry and event duration [16]. In 2014, Allen et al. showed that the equations used by
262 Method 2 were not significantly correlated with measurements made at 32 non-plunger lift wells,
263 although the mean estimate was statistically similar to the mean measured emission. Conversely,
264 measurements at 75 wells with plunger lifts were found to be significantly correlated with the
265 Method 3 estimates (r^2=0.08, p=0.015), but the mean estimate was 44% lower than the mean
266 measured emission. Allen's data illustrates that the accuracy of the estimates provided to the
267 GHGRP is limited even if the parameters required by the method are well known.

268

269 Zaimes et al recently showed that the GHGRP data is too limited to quantitatively represent the
270 range of emissions associated with unloading events [14]. To improve on the GHGRP data for
271 Monte Carlo modeling, Zaimes combined data from three sources – *DIDesktop*, Allen et al.
272 unloading measurement campaign, and the GHGRP. Zaimes' method relies on the GHGRP
273 Method 2 and 3 correlation equations to estimate unloading emissions based on well
274 characteristics and does not account for the systematic errors in those methods that Allen's
275 measurements suggest. However, Zaimes' approach enables Monte Carlo modeling of the
276 uncertainty in emissions while the GHGRP data does not provide for the distribution of well
277 parameters that result in the reported emission estimates.

278

279 Despite these limitations, the base-case simulations presented here use GHGRP data to represent
280 the current emission estimate available to regulators. The presence of unloading events can affect
281 simulation results by triggering site-level survey programs to dispatch ground crews. However,
282 the frequency of unloading events in this simulation—an average of one 34-minute event every
283 63 days at wells with plungers—results in a low probability of an unloading event affecting an
284 LDAR program. Users of the FEAST model attempting to evaluate LDAR programs in basins
285 with significant unloading events should considering incorporating basin-specific data on
286 unloading emisisons to improve the accuracy of results.

287

S2.5 Leak production rate and UDIM repair rate

The leak production rate is a primary driver of uncertainty, as shown in the sensitivity analysis. The base case leak production rate of 3 leaks per site per year used in this work is within the range of previously published estimates and empirically supported by a new estimate based on the regulated OGI survey reports released by the Colorado Department of Public Health and Environment (CDPHE).

The CDPHE requires OGI surveys at all production sites monthly, quarterly, semi-annually, or annually depending on the size and location of the site. We divided the number of emissions discovered at each survey frequency by the time between surveys, then computed the average across all survey frequencies weighted by the number of sites. The resulting average leak production rate estimate in this case was 2 leaks per site per year.

Unchecked, the leak production rate estimated above results in unrealistic growth in emissions over timescales longer than a year. In keeping with prior publications, we assume that an undirected maintenance process results in a steady state number of emissions equal to that observed in the empirical emission data set. We explore sensitivity of the results to both the UDIM repair rate and the leak production rate in Section S4.

S3. LDAR programs

LDAR program simulations require specifying three classes of variables:
1. Detection technology characteristics
2. Program implementation protocols
3. Repair protocols

Each of these classes of variables are described below.

S3.1.1 Detection technology characteristics

Detection technologies in FEAST are defined by their probability of detecting emissions and their ability to disaggregate overlapping emissions. Depending on the technology, the probability of detection may depend on flux, wind speed, operator experience, and other exogenous parameters. Prior modeling efforts used a Gaussian plume dispersion model, empirical wind speed distributions, and a range of atmospheric stability classes to determine the concentration of emitted gases in the volume surrounding an emission source. The concentration profile was then used to calculate the signal in a variety of detection technologies [17]. More recently, empirical, one dimensional probability of detection curves based on emission rate were favored over plume modeling [18]. The empirical approach is powerful because it uses measured technology performance directly. However, to effectively model field performance of new technologies, the probability of detection curve must represent the range of conditions that will be realized in the field. This will result in a much broader probability of detection curve than can be measured at a test site under a single set of conditions. The effect of meteorology, user experience and other variables on probability of detection will need to be accounted for in order to extrapolate from test conditions to field applications [19]–[21].

When the data are available, detection technologies should be modelled using probability of detection surfaces that capture the variables most likely to impact detection for each technology. However, adding variables to technology models will introduce the "curse of dimensionality" to

333   testing requirements. As suggested by Barchyn et al. [19], requiring that detection technologies
334   are only applied under a particular range of conditions would limit the need for testing. Future
335   versions of FEAST will support probability of detection surfaces with two independent variables
336   as well as operating envelopes.
337
338   In this work, the probability of detection for a given flux is calculated according to Equation
339   (*S3)*, where *f* is the emission flux, μ is the log of the median detection threshold – the emission
340   rate with a 50% probability of detection – and λ is a fitting parameter that defines the slope of the
341   curve. The median detection threshold is taken from recently published controlled release tests of
342   methane detection technologies [18], [20], [22]

$$p(d|f) = 0.5 + 0.5 * \text{erf}\left(\frac{ln(f) - \mu}{\sqrt{2}\lambda}\right) \tag{S3}$$

343   Figure S2 shows the PoD curves used in simulations presented in Figures 1-2 in the main text.
344
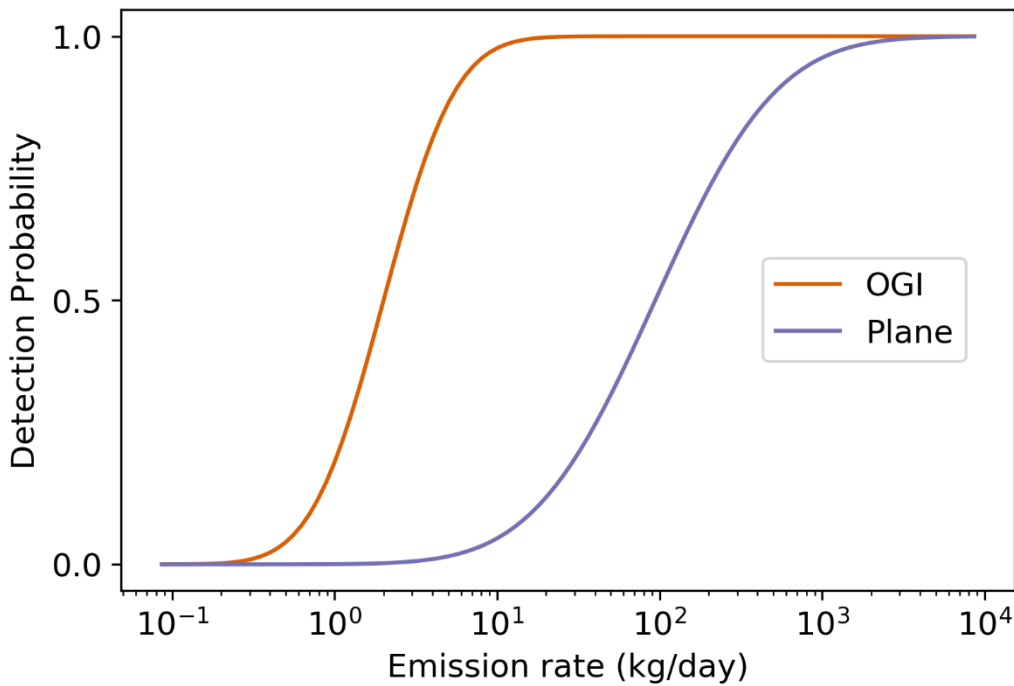
345
346   *Figure S2 Probability of detection curves for the OGI (orange) and the plane-based (purple) technology*
347   *modeled in this study.*

348   S3.1.2   Program implementation protocols
349   LDAR program implementation protocols specify how a detection technology will be used.
350   These protocols include the survey frequency, and relationships between detection methods. For
351   the Plane + OGI programs represented here, the LDAR program specifies that an OGI detection
352   method should be dispatched at any site where the plane detects emissions. LDAR protocols also
353   specify which repair methods should be dispatched if an OGI detection method identifies a
354   repairable emission.
355

356 ### S3.1.3 Repair protocols
357 Repair methods cause an emission to cease and are characterized by the time between when they
358 are called and when the repair occurs. Component level surveys are assigned a 1 day delay
359 between detection and repair, while site level surveys are assigned a 1 week delay.
360
361 ### S3.2 Calculating mitigation costs
362 FEAST calculates costs based on the survey speed (components/hour) and hourly cost in the case
363 of component-level surveys. Costs for site level methods are calculated based on a cost per site
364 parameter. Repair costs are also assigned to leaks repaired by either UDIM or an LDAR
365 program. The total cost of an LDAR program includes survey costs and the difference in repair
366 costs between the LDAR scenario and the UDIM only scenario. Since most leaks are repaired by
367 UDIM over the course of the three-year simulation, the net repair costs assigned to LDAR
368 programs is small compared to the costs of survey.
369
370 Mitigation cost is calculated as the ratio of total cost to avoided greenhouse gas emissions, as
371 shown in Equation (S4). GWP_{CH_4} is the global warming potential of methane, set to 34 in this
372 case following estimates from the IPCC 5th Assessment Report [23].

$$Mitigation\ cost = \frac{Total\ cost}{Methane\ emissions\ mitigated\ (metric\ ton) \times GWP_{CH_4}} \quad (S4)$$

373

374 # S4. Sensitivity Analysis

375
376 The results of an equivalence analysis are sensitive to the parameters specified in FEAST
377 simulations. In the main text, we highlighted the sensitivity of results to survey frequency in
378 Figure 2, detector sensitivity and survey frequency in Figure 3, and emission distribution skew
379 and detector sensitivity in Figure 4. These figures show that the model is neither linear nor
380 additive: local derivatives of results with respect to one input variable are not indicative of model
381 behavior across the range of possible input values, and the impact on results of changing two
382 input values cannot necessarily be approximated by adding the impact of changing each input
383 value independently. The "one-at-time" style sensitivity analysis presented in previous FEAST
384 publications provides insight into the sensitivity of the model to input parameters near the "base
385 case" scenario but is difficult to use in assessing the overall sensitivity of the model. Allowing
386 multiple input parameters to vary simultaneously provides better representation of the sensitivity
387 of the model to changes in the underlying assumptions [24].
388
389 Our sensitivity analysis is designed to assess the confidence that a regulator could have in an
390 equivalence assessment given the existing data to support global parameters in FEAST. Global
391 parameters refer to parameters that are consistent across all Monte Carlo iterations of a scenario,
392 such as the choice of leak production rate, emission rate distribution, and vent fraction.
393 Specifically, we ask: given realistic uncertainties in global parameters defined for FEAST
394 simulations, how confident can a regulator be that two distinct LDAR programs that appear to be
395 equivalent under the assumptions described for this work would achieve equivalent results in the

396   field? To answer this question, we consider a Plane + OGI program with a survey frequency of
397   9/year, and an OGI program with a survey frequency of 2/year.
398
399   Figure 2 in the main text shows that the mean emission rates are equal for these LDAR programs
400   but there is variability in those emission rates due to several random process included in FEAST.
401   The random processes in FEAST include the Poisson process representing emission creation, the
402   distribution of fugitive emission sizes, and the PoD surface. These processes are inherently
403   probabilistic: with perfect information, a regulator would still expect to see variability in results.
404
405   To these random processes, we now add a distribution for parameters in FEAST that may not be
406   inherently probabilistic but are poorly constrained by available empirical data. We suppose that
407   the LDAR program parameters are known precisely, but the leak production rate, UDIM repair
408   rate, emission distribution, and vent fraction are only constrained by existing empirical data. The
409   range of results gives a quantitative illustration of the confidence that a regulator could have in
410   an equivalence assessment given perfect information about an LDAR program and illustrates the
411   areas where additional empirical data would improve confidence the most.
412

413   ## S4.1 Emission rate distribution
414   Figure 4 showed that the emission rate distribution affects the level of mitigation that LDAR
415   programs can achieve. How confident can a user be in the emission distribution used by FEAST?
416
417   We examine the sensitivity to the component level distribution by invoking different empirical
418   component-level leak distributions. In each iteration of the sensitivity analysis, we randomly
419   select results from one of the five studies listed in
420   . The study used in each iteration is treated as a categorical variable, with equal probability
421   assigned to each study.
422

423   ## S4.2 Leak production rate and UDIM repair rate
424   The leak production rate ($R_f - failures\ per\ component\ per\ day$) and UDIM repair rate
425   ($R_R - repairs\ per\ leak\ per\ day$) are related to each other in FEAST by Equation (S5, where
426    $N_c(t)$ and $N_L(t)$ are the number of components and number of leaks as functions of time (t).
427   The $\langle\ \rangle$ notation indicates an expectation value (i.e., the theoretical average across an infinite
428   number of iterations and timesteps).

$$\langle\frac{dN_L(t)}{dt}\rangle = N_c R_f - N_L(t) R_R \qquad \text{(S5)}$$

429   Setting a boundary condition of $N_L(t=0) = N_{L0}$, we can solve Equation (S5 to derive an
430   expression for $N_L(t)$ as shown in Equation (S6.

$$\langle N_L(t)\rangle = N_{L0} + N_c\frac{R_f}{R_R}(1 - \exp(-R_R t)) \qquad \text{(S6)}$$

431   R_f and R_R could be determined by fitting Equation (S6 to the time evolution of emission counts
432   at production sites (for example, by conducting repeated surveys of the same sites without
433   reporting emission to operators). However, such data are not presently available. Therefore, we
434   developed a range of likely values for R_f and R_R in this sensitivity analysis.
435

436 ### S4.2.1 Leak production rate distribution
437 We developed the likely range for R_f and R_R using LDAR data from periodic surveys of
438 production equipment in Colorado. First, we consider the case in which the UDIM repairs are
439 rare between surveys ($R_R t_s \ll 1$) where t_s is the time between surveys. We also assume that the
440 vast majority of leaks are detected and repaired at each survey ($\langle N_L(t_s) \rangle \gg N_{L0}$). In that case a
441 Taylor expansion of Equation (S6) reveals that $\langle N_L(t_s) \rangle \approx N_c R_f t_s$. Therefore, the leak
442 production rate R_f can be estimated based on the number of leaks detected in periodic surveys if
443 the survey interval and number of components surveyed is known.
444
445 In order to develop a distribution for R_f to use in sensitivity analysis, we consider surveys
446 conducted at different site types and frequencies in Colorado. Specifically, we consider sites
447 surveyed once, twice, four and twelve times per year. The survey frequency required by the state
448 of Colorado depends on the site characteristics (larger sites generally require more frequent
449 surveys) and site location (sites in non-attainment zones require more frequent surveys) [5]. The
450 data are summarized in Table S3. In the sensitivity analysis, each survey frequency is selected
451 with a probability equal to the fraction of total sites included in the reports. In comparison, the
452 leak production rate used for Figures 1-4 in the main text is 3 leaks per site per year, [25] used
453 2.4 leaks per *well* per year, and Fox et al. reported a mean leak production rate estimate of 9.5
454 leaks per site per year [26]. To convert the reported leaks per site to a component-level leak
455 production rate, we divide by 1235 components per site (assumes 650 components per well and
456 an average of 1.9 wells per site).
457
458 *Table S3 Summary of data reported in LDAR surveys regulated by CDPHE*

Survey frequency (surveys per year)	Leaks identified per site per year	Inspections that occurred	Approximate number of sites based on number of inspections
1	0.8	4246	4246
2	0.7	4907	4907
3	4.2	3766	942
4	12.8	10914	910

459
460
461 The leak production rate estimated by long survey frequencies of six months or one year in Table
462 S3 likely underestimate the leak production rate to due to UDIM repairs that occur between
463 surveys. Conversely, the leak production rate in monthly surveys is likely overestimated due to
464 the regulator requiring monthly surveys only at sites expected to have high emissions. Therefore,
465 the range indicated by Table S3 may exaggerate the range of likely component-level leak
466 production rates.
467
468 ### S4.3 UDIM repair rate distribution
469 In Figures 1-4 of the main text, the UDIM repair rate was set to guarantee that in the absence of
470 an LDAR program, the frequency of emissions in the simulation tended toward the frequency of
471 emissions observed in the included field studies. Here, we choose the UDIM repair rate from a
472 triangular distribution. The inverse of the UDIM repair rate provides the mean duration of an

473   emission under UDIM. The mode of the triangular distribution is set to a mean duration of 208
474   days, the same value used in simulations for the main text. The minimum UDIM emission
475   duration is set to 100 days, and the maximum is set to three years.
476

477   ### S4.4 Vent fraction
478   In the main text, the vent fraction excluding unloading events was set to 46%. Unloading events
479   were rare in these simulations, increasing the overall vent fraction to 47% despite their large
480   emission rate. Prior studies have identified vented emissions contributing between 55% and 90%
481   of total emissions (with the highest vent fractions coming from compressor stations rather than
482   well sites) [4], [27]–[29]. In this sensitivity analysis, we choose the vent fraction from a uniform
483   distribution ranging from 30 to 60%. The high end of the vent fraction range is consistent with
484   emission fractions observed at well sites, and the low end of the range allows for the possibility
485   that some emissions classified as vents (such as fugitive tank emissions) would be mitigated in a
486   practical LDAR program.
487

488   ### S4.5 Confidence in equivalence assessments
489   We define an equivalence metric ϕ in Equation (S7) to quantify the equivalence between two
490   proposed LDAR programs. F denotes the total fugitive emissions under an LDAR program. The
491   subscript $plane$ indicates the Plane + OGI LDAR program with a survey frequency of 9/year and
492   median detection threshold of 94 kg/day, while the subscript OGI refers to the component level
493   survey with a frequency of 2/year and a detection threshold of 2 kg/day.

$$\phi = \frac{F_{plane} - F_{OGI}}{F_{plane} + F_{OGI}} \qquad (S7)$$

494

495   Values of $\phi < 0$ imply thate the Plane + OGI program reduces emissions more than the OGI
496   program while $\phi > 0$ implies that the OGI program outperforms the Plane + OGI program. ϕ is
497   bounded between -1 and 1. When the two programs achieve equal mitigation, $\phi = 0$.
498

499   Figure S3 shows a histogram of ϕ resulting from 10,000 iterations of FEAST with values of the
500   leak production rate, emission distribution, UDIM repair rate and vent fraction drawn from the
501   distributions described above. 12% of the iterations result in the Plane + OGI program achieving
502   equivalent mitigation to the OGI program. This implies that, although the assumptions presented
503   in the main text of the paper result in the Plane + OGI program achieving equal mitigation to the
504   OGI program at these survey frequencies, we cannot be confident in that result given existing
505   uncertainty in the leak production rate and emission distribution. The following section
506   investigates the type of empirical data that would be most valuable to increasing confidence in
507   equivalence evaluations.
508
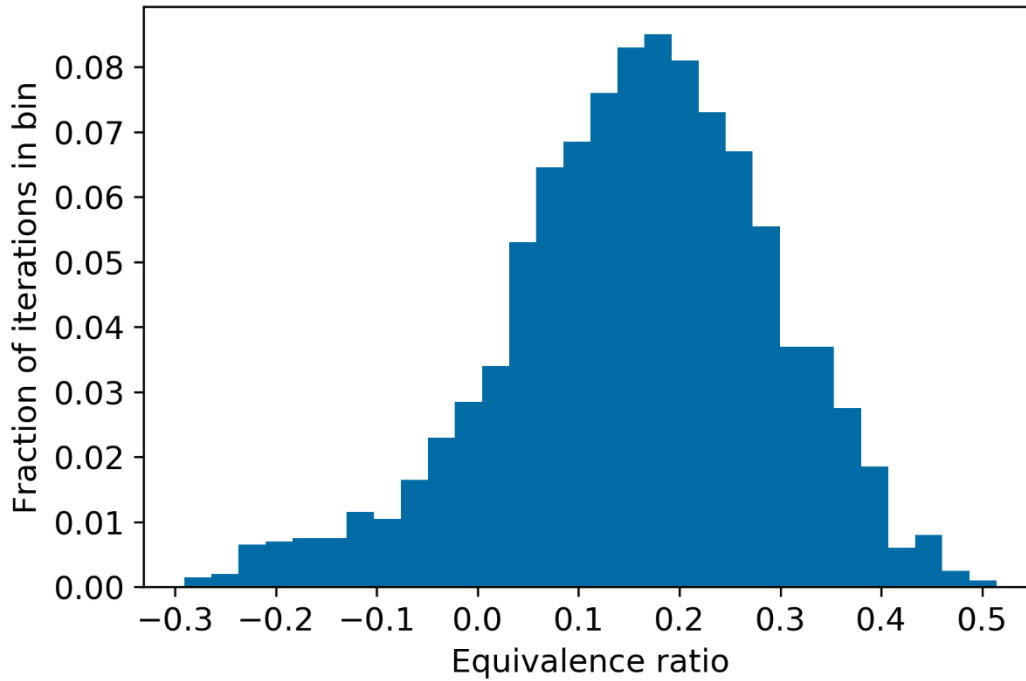
509
510 *Figure S3 Distribution of the equivalence ratio while varying input parameters to FEAST.*

S4.6 Sensitivity of results to input parameters

512 The following figures illustrate the sensitivity of the model to the four parameters considered in
513 this section. We find the greatest value will come from reducing uncertainty in the leak
514 production rate, followed by the emission distribution. The results have little sensitivity to the
515 vent fraction.
516
517 Figure S4 shows the distribution of the equivalence metric under different leak production rates.
518 The distributions show that the Plane + OGI program performs better in comparison to the OGI
519 program (the equivalence metric decreases) as the leak production rate increases. However, there
520 is significant overlap between the distributions: other sources of uncertainty are also important.
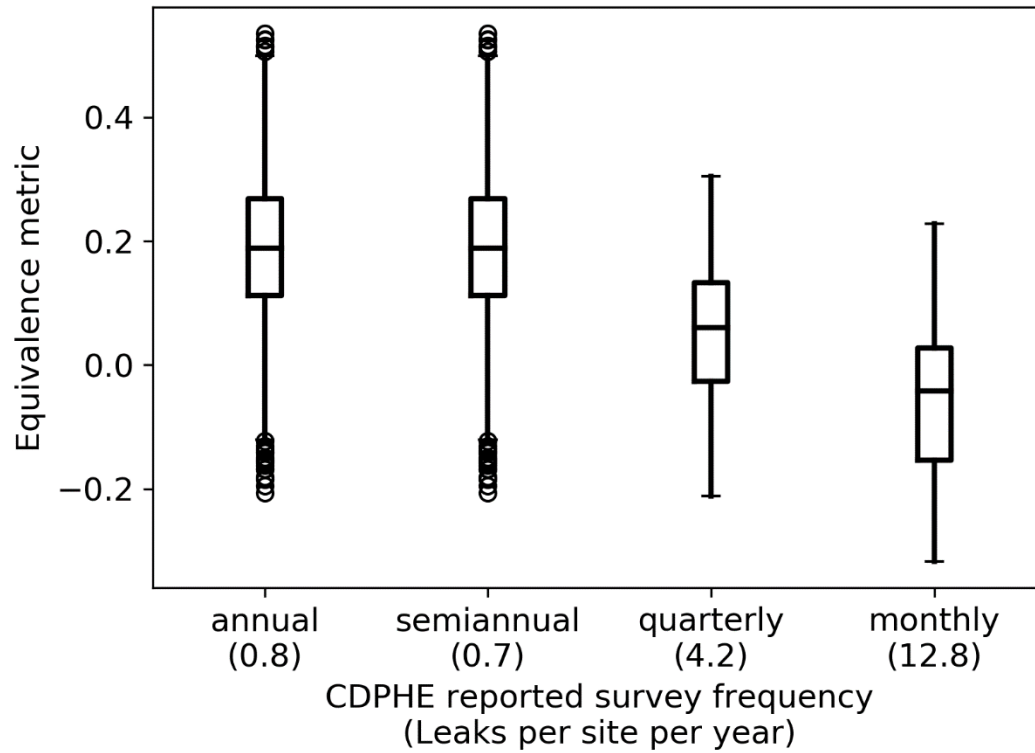
521
522 *Figure S4 Distribution of the equivalence ratio when the leak production rate is estimated using results*
523 *from OGI surveys regulated by the Colorado Department of Public Health and Environment (CDPHE).*
524 *Different survey frequencies are applied to different production sites, resulting in distinct leaks per site per*
525 *year estimates when the data are separated by survey frequency.*

526 Figure S5 shows the distribution of the equivalence metric under different emission distributions.
527 The data show that the results are sensitive to the emission distribution chosen for the
528 simulations. To develop fair equivalence metrics, regulators must choose an emission
529 distribution that accurately represents their facilities.
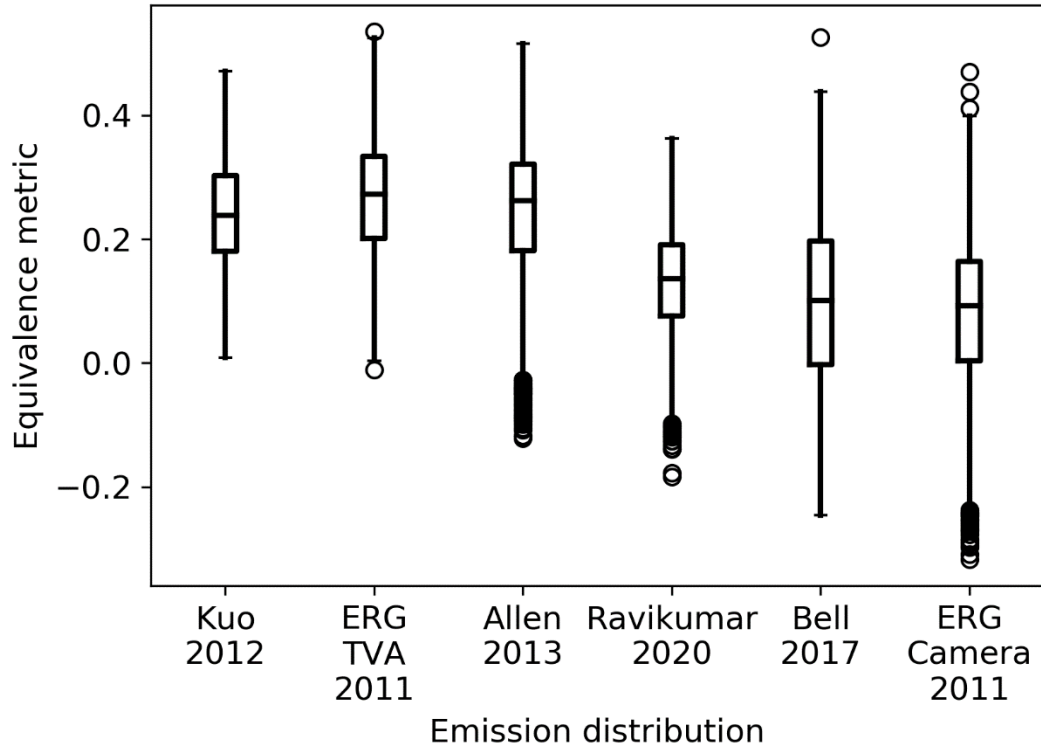
530
531   *Figure S5 Distribution of the equivalence metric under different emission distributions. Emission*
532   *distributions are in order of increasing mean emission rate.*

533   Figure S6 shows results from all monte carlo iterations plotted against the UDIM leak lifetime
534   chosen for each iteration (1/UDIM repair rate). We see that the variance is dominated by other
535   sources of uncertainty, but there is a correlation between UDIM leak lifetime and Equivalence
536   metric (r-value of 0.082 and p-value <0.001). The impact of the UDIM leak lifetime is limited
537   because most emissions are repaired by the LDAR program in both the OGI and the Plane + OGI
538   cases rather than by the UDIM process.
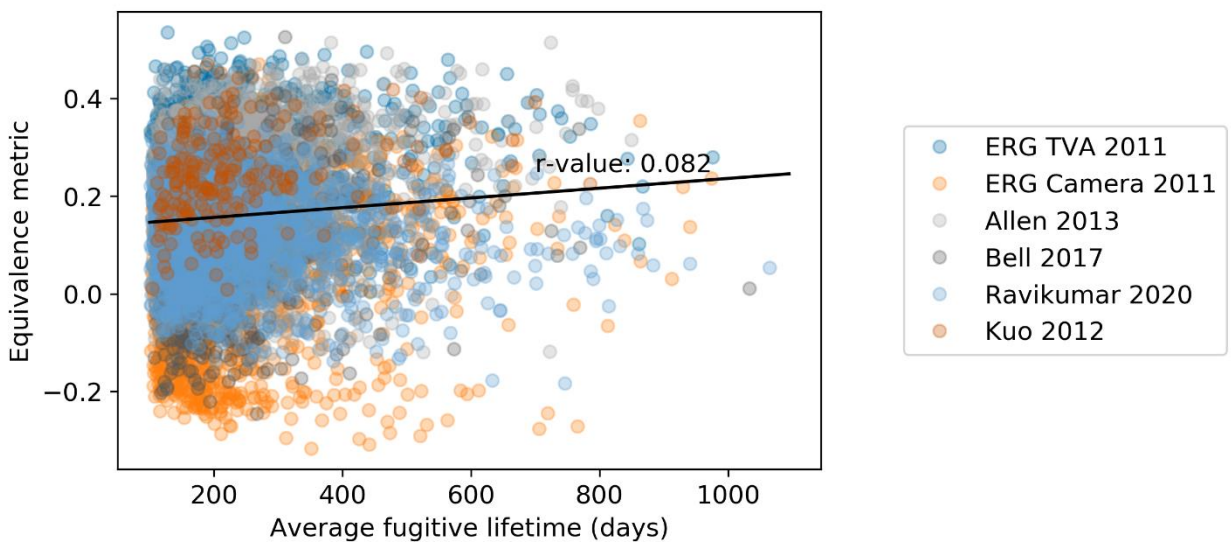
539
540   *Figure S6 Equivalence metric of all iterations plotted against the expected leak lifetime under UDIM. The*
541   *best linear fit to the data is plotted along with the correlation coefficient of the fit.*

542 Finally, Figure S7 shows results from all Monte Carlo iterations plotted against the vent fraction.
543 The data suggest that equivalence, in this case, is weakly dependent on the vent fraction in the
544 range tested (p-value of 0.1). This result is due to the Plane + OGI flagging the same sites for
545 follow up surveys regardless of whether emissions are classified as fugitive or vent. Increasing
546 the vent fraction decreases the emission mitigation from those flagged sites equally for both
547 types of LDAR program.
548
549 To illustrate the impact of vent fraction on the equivalence ratio, consider the example in Table
550 S4. There are two sites in the example. In every case, there are two emissions at Site 1 (0.2 and
551 1.0 g/s) and three emissions at Site 2 (0.2, 0.1 and 0.01 g/s). The emissions are classified as vents
552 or leaks in four distinct scenarios. In case 1, all of the emissions are classified as fugitive
553 emissions. In cases 2-4, two of the emissions are classified as vents. We imagine a tiered LDAR
554 program that flags all sites with emissions >1.0 g/s for follow up action. We also consider a
555 component level inspection program that repairs all fugitive emissions > 0.05 g/s. In short, the
556 tiered program repairs all fugitive emissions at Site 1, and the component level program repairs
557 all fugitive emissions except the 0.01 g/s emission.
558
559 Table S4 shows that the effect of the vent fraction on the equivalence ratio depends on which
560 emissions are classified as vents. Case 1 has a vent fraction of 0 resulting in an equivalence ratio
561 of 0.94. Cases 2-4 have higher vent fractions, but the equivalence ratio can be greater than, less
562 than or equal to the equivalence ratio of Case 1. The effect of the vent fraction on the
563 equivalence ratio depends on the relative sizes of the emissions classified as vents and fugitive
564 emissions.
565
566 *Table S4 Example of the impact of vent fraction on equivalence ratio*

	Site 1 emissions (g/s)		Site 2 emissions (g/s)		Number of vents	Vent fraction	Equivalence metric
	Fugitive	Vent	Fugitive	Vent			
Case 1	0.2, 1.0	-	0.2, 0.1, 0.01	-	0	0	0.94
Case 2	1.0	0.2	0.1, 0.01	0.2	2	26%	0.83
Case 3	-	0.2, 1.0	0.2, 0.1, 0.01	-	2	79%	0.94
Case 4	0.2, 1.0	-	0.1	0.2, 0.01	2	14%	1.0

567
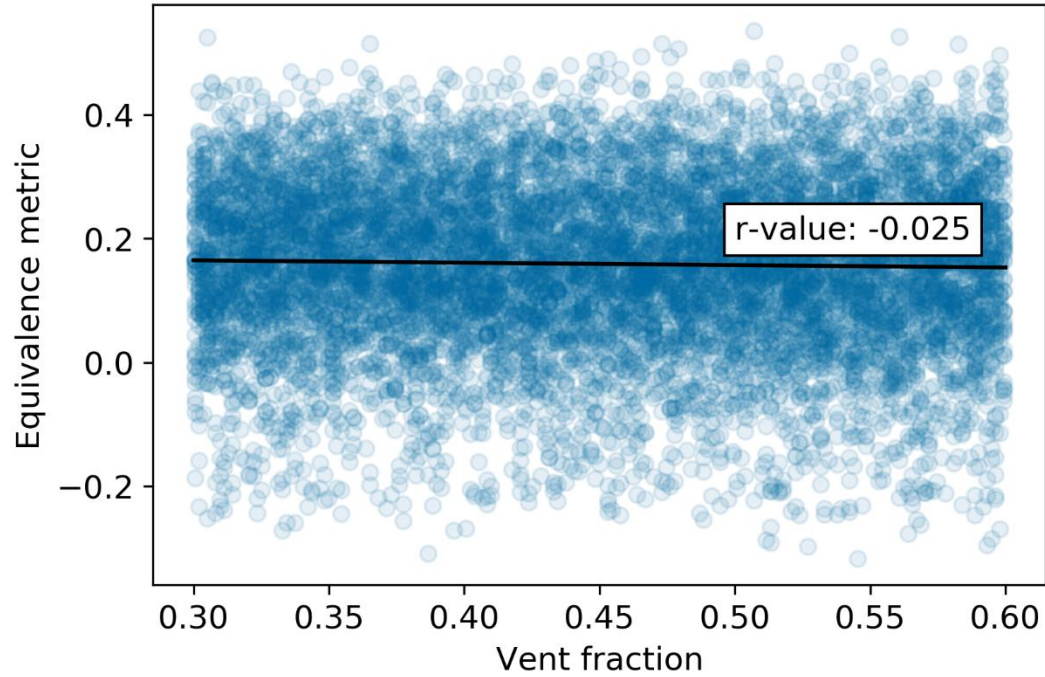
568
569 *Figure S7 Equivalence metric of all iterations plotted against the vent fraction under UDIM. The best*
570 *linear fit to the data is plotted along with the correlation coefficient of the fit.*

571 In order to assess the value of reducing uncertainty in these four global parameters, we adopt a
572 first order sensitivity index S_i [24]. S_i is defined by Equation (S8). V_{X_i} is a variance operator
573 with one parameter (i) held constant. $E_{X_{\sim i}}$ is an expectation value operator across all variables
574 except i. ϕ is the equivalence ratio defined in Equation (S7), and X is the set of input parameters
575 varied for the sensitivity analysis.

$$S_i = \frac{V_{X_i}(E_{X_{\sim i}}(\phi|X_i))}{V(\phi)} \tag{S8}$$

576 Figure S8 shows S_i for the vent fraction, UDIM repair rate, leak production rate and emission
577 distribution. Eliminating uncertainty in the parameter with the largest S_i would cause the greatest
578 decrease in variance of the equivalence ratio $V(\phi)$. Therefore, reducing uncertainty in the leak
579 production rate will have the greatest impact on uncertainty in equivalence analyses.

19
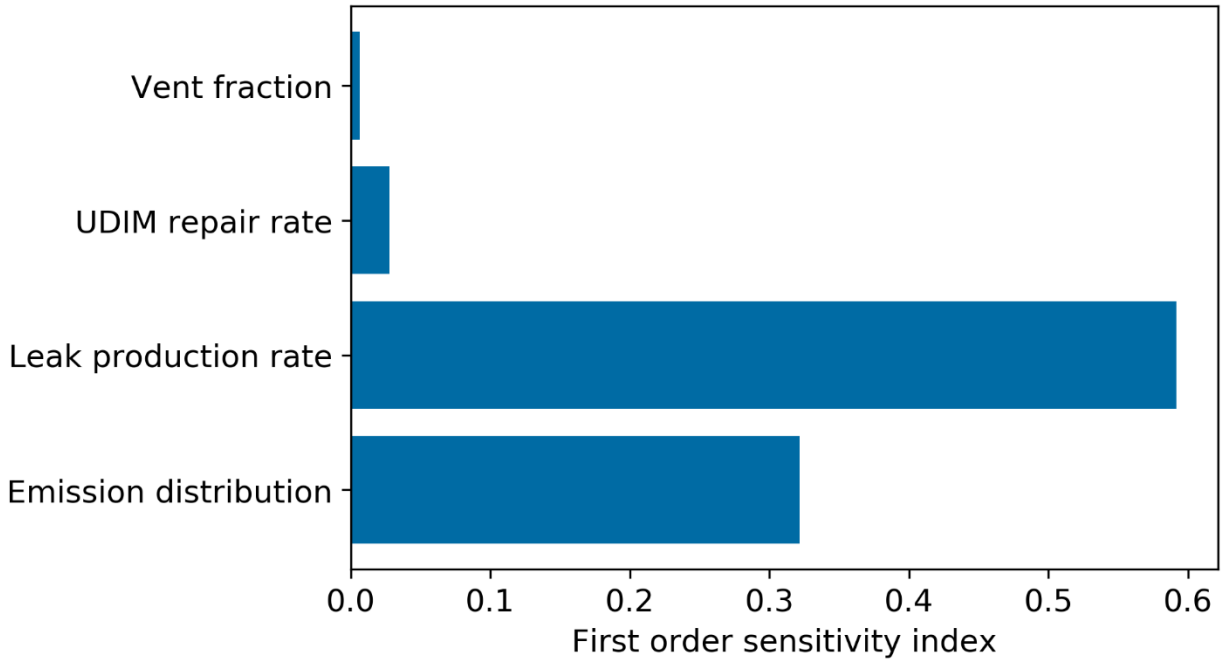
580
581 *Figure S8 Sensitivity index of the four parameters tested in the sensitivity analysis.*

582

S4.7 Emissions variability versus detection variability

583
584 The uncertainty in FEAST *emission* estimates is distinct from the uncertainty in *equivalency*
585 estimates. Figure S9 shows the average emission rate in 100 iterations of FEAST with the same
586 emission scenario. A UDIM scenario, a biannual OGI survey and a biannual Plane + OGI survey
587 are considered. The emission rates shown are averaged across the 3-year simulation period and
588 100 well pads simulated in each iteration. In the UDIM scenario, the average fugitive emission
589 rate ranges from 7 to 19 kg/day-site. In the Plane + OGI scenario, the rate ranges from 5 to 11
590 kg/day-site and in the OGI scenario the rate ranges from 3 to 7 kg/day-site. The ranges of the
591 average site-level emissions overlap across the three scenarios. However, the ranking of the
592 programs is consistent across each individual iteration – i.e., the OGI survey results in the least
593 fugitive emissions, followed by the Plane + OGI and then the UDIM scenario. Figure S9 shows
594 uncertainty in total emission estimates does not necessarily cause proportionate uncertainty in
595 comparisons between LDAR programs. That is, the relative performance of different programs is
596 significantly less uncertain than the range of fugitive emissions observed.

20
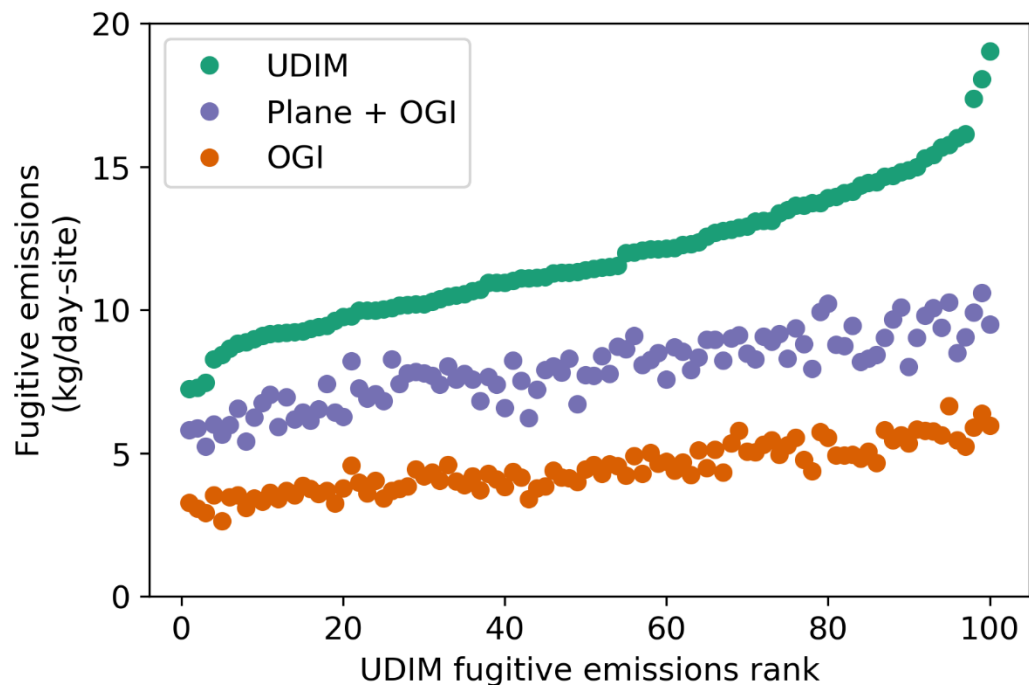
597
598 *Figure S9 Average site-level fugitive emission rate under distinct LDAR scenarios, sorted by the UDIM*
599 *fugitive emission rate. Results represent average emissions across a 3-year simulation period over 100*
600 *well pads.*

601

602
603
604
605
606

S5.   Supporting Information References

608 [1]   COGCC, "COGCC/Data Downloads/GIS/Well Surface Location Data (Updated
609   Daily)/Well Spots (APIs)," *Colorado Oil and Gas Conservation Commission*, 2019.
610   https://cogcc.state.co.us/documents/data/downloads/gis/WELLS_SHP.ZIP (accessed Jan.
611   13, 2020).
612 [2]   M. Omara *et al.*, "Methane Emissions from Natural Gas Production Sites in the United
613   States: Data Synthesis and National Estimate," *Environ. Sci. Technol*, vol. 52, p. 51, 2018,
614   doi: 10.1021/acs.est.8b03535.
615 [3]   "Oil and Natural Gas Sector : Standards for Crude Oil and Natural Gas Facilities:
616   Background Technical Support Document for the Proposed New Source Performance
617   Standards 40 CFR Part 60, subpart OOOOa." EPA, Chapel Hill, NC, 2016, [Online].
618   Available: https://beta.regulations.gov/document/EPA-HQ-OAR-2010-0505-7631.
619 [4]   A. P. Ravikumar *et al.*, "Repeated leak detection and repair surveys reduce methane
620   emissions over scale of years," *Environ. Res. Lett.*, 2020, doi: 10.1088/1748-9326/ab6ae1.
621 [5]   *Control of Ozone via Ozone Precursors and Control of Hydrocarbons via Oil and Gas*
622   *Emissions*. 2019.

623   [6]   D. Allen *et al.*, "Measurements of methane emissions at natural gas production sites in the
624   United States David," *Proc. Natl. Acad. Sci.*, vol. 110, no. 44, pp. 18025–18030, Sep.
625   2013, doi: 10.1073/pnas.1315099110.
626   [7]   "City of Fort Worth Natural Gas Air Quality Study," Fort Worth, TX, 2011. [Online].
627   Available: http://fortworthtexas.gov/uploadedFiles/Gas_Wells/AirQualityStudy_final.pdf.
628   [8]   J. Kuo, "Final project report estimation of methane emissions from the California Energy
629   Commission," 2012. doi: 500-09-007.
630   [9]   C. S. Bell *et al.*, "Comparison of methane emission estimates from multiple measurement
631   techniques at natural gas production pads," *Elem Sci Anth*, vol. 5, no. 0, p. 79, Dec. 2017,
632   doi: 10.1525/elementa.266.
633   [10]   U.S. Environmental Protection Agency, "Inventory of U.S. Greenhouse Gas Emissions
634   and Sinks: 1990-2018 – EPA 430-R-20-002," Apr. 2020. Accessed: Aug. 13, 2020.
635   [Online]. Available: https://www.epa.gov/ghgemissions/inventory-us-greenhouse-gas-
636   emissions-and-sinks.
637   [11]   D. T. Allen *et al.*, "Methane Emissions from Process Equipment at Natural Gas
638   Production Sites in the United States: Pneumatic Controllers," 2014, doi:
639   10.1021/es5040156.
640   [12]   A. R. Brandt, G. A. Heath, and D. Cooley, "Methane Leaks from Natural Gas Systems
641   Follow Extreme Distributions," 2016, doi: 10.1021/acs.est.6b04303.
642   [13]   U.S. Environmental Protection Agency, "Facility Level Information on Greenhouse Gases
643   Tool," 2017. https://ghgdata.epa.gov/ghgp/main.do#/listFacilityForBasin/?q=Find a
644   Facility or Location&bs=540&fid=&sf=11001000&lowE=-
645   20000&highE=23000000&g1=1&g2=1&g3=1&g4=1&g5=1&g6=0&g7=1&g8=1&g9=1
646   &g10=1&g11=1&g12=1&s1=0&s2=0&s3=0&s4=0&s5=0&s6=0&s7=0&s8=0&s9=1&s1
647   0=0& (accessed Oct. 23, 2019).
648   [14]   G. G. Zaimes *et al.*, "Characterizing Regional Methane Emissions from Natural Gas
649   Liquid Unloading," 2019, doi: 10.1021/acs.est.8b05546.
650   [15]   *Mandatory Greenhouse Gas Reporting Subpart W--Petroleum and Natural Gas Systems*.
651   US, 2020.
652   [16]   *Mandatory Greenhouse Gas Reporting Subpart W--Petroleum and Natural Gas Systems:
653   Calculating GHG Emisions*. 2020.
654   [17]   C. E. Kemp, A. P. Ravikumar, and A. R. Brandt, "Comparing Natural Gas Leakage
655   Detection Technologies Using an Open-Source 'virtual Gas Field' Simulator," *Environ.
656   Sci. Technol.*, vol. 50, no. 8, 2016, doi: 10.1021/acs.est.5b06068.
657   [18]   A. P. Ravikumar, J. Wang, M. Mcguire, C. S. Bell, D. Zimmerle, and A. R. Brandt, "Good
658   versus Good Enough? Empirical Tests of Methane Leak Detection Sensitivity of a
659   Commercial Infrared Camera," *Environ. Sci. Technol*, vol. 52, 2018, doi:
660   10.1021/acs.est.7b04945.
661   [19]   T. E. Barchyn, C. H. Hugenholtz, and T. A. Fox, "Plume detection modeling of a drone-
662   based natural gas leak detection system," *Elem Sci Anth*, vol. 7, no. 1, p. 41, Oct. 2019,
663   doi: 10.1525/elementa.379.
664   [20]   D. Zimmerle, T. Vaughn, C. Bell, K. Bennett, P. Deshmukh, and E. Thoma, "Detection
665   Limits of Optical Gas Imaging for Natural Gas Leak Detection in Realistic Controlled
666   Conditions," *Environ. Sci. Technol.*, vol. 54, no. 18, pp. 11506–11514, 2020, doi:
667   10.1021/acs.est.0c01285.
668   [21]   T. A. Fox, T. E. Barchyn, D. Risk, A. P. Ravikumar, and C. H. Hugenholtz, "A review of

669   close-range and screening technologies for mitigating fugitive methane emissions in
670   upstream oil and gas," *Environ. Res. Lett.*, vol. 14, no. 5, p. 053002, Apr. 2019, doi:
671   10.1088/1748-9326/ab0cc3.
672 [22] A. Ravikumar *et al.*, "Single-blind Inter-comparison of Methane Detection Technologies--
673   Results from the Stanford/EDF Mobile Monitoring Challenge," 2019, [Online]. Available:
674   https://doi.org/10.1525/elementa.373.
675 [23] G. Myhre *et al.*, "Chapter 8: Anthropogenic and Natural Radiative Forcing," in *Climate*
676   *Change 2013: The Physical Science Basis. Contribution of Working Group I to the Fifth*
677   *Assessment Report of the Intergovernmental Panel on Climate Change*, T. F. Stocker, D.
678   Qin, G.-K. Plattner, M. Tignor, S. K. Allen, J. Boschung, A. Nauels, Y. Xia, V. Bex, and
679   P. M. Midgley, Eds. Cambridge, United Kingdom and New York, NY, USA, 2013, pp.
680   659–740.
681 [24] A. Saltelli and P. Annoni, "How to avoid a perfunctory sensitivity analysis," *Environ.*
682   *Model. Softw.*, vol. 25, pp. 1508–1517, 2010, doi: 10.1016/j.envsoft.2010.04.012.
683 [25] C. E. Kemp, A. P. Ravikumar, and A. R. Brandt, "Comparing Natural Gas Leakage
684   Detection Technologies Using an Open-Source Virtual Gas Field Simulator," *Environ.*
685   *Sci. Technol*, 2016, doi: 10.1021/acs.est.5b06068.
686 [26] T. A. Fox, M. Gao, T. E. Barchyn, Y. L. Jamin, and H. Chris, "An agent-based model for
687   estimating emissions reduction equivalence among leak detection and repair programs,"
688   pp. 1–44.
689 [27] M. R. Johnson, D. R. Tyner, S. Conley, S. Schwietzke, and D. Zavala-Araiza,
690   "Comparisons of Airborne Measurements and Inventory Estimates of Methane Emissions
691   in the Alberta Upstream Oil and Gas Sector," 2017, doi: 10.1021/acs.est.7b03525.
692 [28] D. R. Johnson, A. N. Covington, and N. N. Clark, "Methane Emissions from Leak and
693   Loss Audits of Natural Gas Compressor Stations and Storage Facilities," *Environ. Sci.*
694   *Technol*, vol. 49, p. 35, 2015, doi: 10.1021/es506163m.
695 [29] D. Zimmerle *et al.*, "Methane Emissions from Gathering Compressor Stations in the
696   U.S.," *Environ. Sci. Technol.*, vol. 54, no. 12, pp. 7552–7561, Jun. 2020, doi:
697   10.1021/acs.est.0c00516.
698